

**Deliverable Report for Grant Agreement Number 760813****Deliverable 1.5****Environmental fate and dosimetry in relevant environmental compartments****Due date of deliverable: 30/06/2020****Actual submission date: 09/09/2020****Lead beneficiary for this deliverable: UNAMUR**

Dissemination Level:		
PU	Public	X
PP	Restricted to other programme participants (including the Commission Services)	
RE	Restricted to a group specified by the consortium (including the Commission Services)	
CO	Confidential, only for members of the consortium (including the Commission Services)	

## TABLE OF CONTENTS

<b>1. DESCRIPTION OF TASK.....</b>	<b>3</b>
<b>2. DESCRIPTION OF WORK &amp; MAIN ACHIEVEMENTS.....</b>	<b>4</b>
<b>2.1 Physicochemical characterisation of NPs in realistic ecotox exposure conditions .....</b>	<b>4</b>
2.1.1 Brünauer, Emmett and Teller (BET) measurements .....	4
2.1.2 X-ray photoelectron spectroscopy (XPS) measurements.....	5
2.1.3 Transmission Electron Microscopy (TEM) measurements.....	7
2.1.4 Effective density measurements .....	10
<b>2.2 Evaluation of the ecotox testing water column .....</b>	<b>12</b>
2.2.1 Experimental part.....	12
2.2.1.1 Materials.....	12
2.2.1.2 Sample preparation.....	12
2.2.1.3 Colloidal characterisation.....	13
2.2.1.4 Sedimentation study.....	13
2.2.1.5 Analytic measurements.....	14
2.2.2 Size, Zeta pot in eco-tox media.....	14
2.2.2.1 Zinc oxide colloidal stability .....	14
2.2.2.2 Titanium dioxide colloidal stability.....	19
2.2.2.3 TiO <sub>2</sub> in Elendt M7 .....	19
2.2.2.4 TiO <sub>2</sub> in Egg Water .....	21
2.2.2.5 Cerium dioxide colloidal stability.....	22
2.2.2.6 Conclusions .....	23
2.2.3 Height concentration profiles in eco-tox media .....	24
2.2.3.1 TiO <sub>2</sub> in Elendt M7 .....	24
2.2.3.2 TiO <sub>2</sub> in Egg Water .....	25
2.2.3.3 CeO <sub>2</sub> in Elendt M7.....	26
2.2.3.4 Conclusions .....	27
2.2.4 Particle size distribution via CLS measurements.....	27
2.2.5 Turbiscan measurements and determination of sedimentation rate.....	36
<b>2.3 Dosimetry analysis of ecotox suspensions.....</b>	<b>38</b>
2.3.1 Total metal concentrations in the Egg Water .....	39
2.3.2 Particle sizes in Egg Water.....	41
2.3.3 Dissolution Analysis in Egg Water.....	41
2.3.4 Total metal content in exposed zebrafish embryo-larvae.....	42
2.3.5 Fate assessment of nZnO for long-term Daphnia magna tests.....	43
2.3.6 Fate assessment of nTiO <sub>2</sub> for long-term Daphnia magna tests .....	52
2.3.7 Fate assessment of nTiO <sub>2</sub> for long-term Egg water tests .....	55
2.3.8 Characterisation of Zebra fish eggs exposed to NPs .....	58
2.3.9 Overall conclusions .....	62
<b>3. DEVIATIONS FROM THE WORKPLAN .....</b>	<b>62</b>
<b>4. PERFORMANCE OF THE PARTNERS .....</b>	<b>64</b>
<b>5. CONCLUSIONS.....</b>	<b>64</b>
<b>6. ANNEX - REFERENCES.....</b>	<b>64</b>

## 1. Description of task

Environmental fate and dosimetry of Tier 1 ENM will be established in environmental matrices defined in WP5 (water and/or sediment-based systems). CLS, XPS, ( $\mu$ )PIXE and ICPMS techniques will be used to determine size, concentration, uptake, biodistribution and mapping of Tier 1 ENM (UNamur, USC). The  $\mu$ PIXE technique is an ion beam technique that allows detection and mapping of elements at submicron sizes with higher sensitivity than EDX, and is particularly powerful to assess ENM in an organ or complex biological matrix. This technique will be used to obtain a mapping of ENM/agglomerates in organs and/or tissues from selected organisms and experiments provided by WP5 (UNamur). A strong link between Task 1.5 with WP5 and WP6 will be established; WP5 will provide the appropriate environmental samples to support analysis in this task; later, obtained data will be fed into WP6 to support the environmental in silico dosimetry modelling (Task 6.4). Special attention will be given to key properties influencing fate and transport of ENM in suspension, among them: size, degree of agglomeration and effective density (BASF, UNamur, USC). A transgenic fish model for oxidative stress (fluorescence, via the electrophile response element pathway) will also be employed to understand how the different materials and matrices affect their bioavailability in an intact organism (UNEXE). SOPs will be developed together with WP5 and will be inputted to T1.6.

## 2. Description of work & main achievements

### 2.1 Physicochemical characterisation of NPs in realistic ecotox exposure conditions

UNamur was focused on the characterisation of engineered nanomaterials (ENMs) using multiple analytical characterisation tools. Properties of ENMs, under realistic exposure conditions, are required to understand fate and dosimetry in relevant environmental compartments. Physicochemical intrinsic properties of ENMs, such as: surface area, morphology, chemical surface composition and primary size, were evaluated. The behaviour of ENMs in water or biological matrices were also studied. Exposure properties, such as: particle size distribution, agglomeration state, sedimentation rate and effective density, were determined in relevant conditions.

Titanium dioxide (TiO<sub>2</sub> NM-105), Silicon dioxide (SiO<sub>2</sub> NM-200), Zinc oxide naked (ZnO NM-110), coated with triethoxycapryl silane (ZnO NM-111) and Multiwall carbon nanotubes (MWCNT NM-402) were evaluated. Measurements are compared with the data provided by several European laboratories which have participated in the NANOGENOTOX Joint Action, as part of the launch of the "Testing a Representative set of Manufactured Nanomaterials" (program coordinated by the Joint Research Centre).<sup>1-4</sup>

#### 2.1.1 Brünauer, Emmett and Teller (BET) measurements

Specific surface area, total and micropore volume parameters were determined using BET instrument (ASAP 2010, Micromeritics) and are listed in

**Table 1** and **Table 2** respectively. BET surface area values of all ENMs were found to be lower than the JRC data. Differences could be in part attributed to the type of instrument used to perform the analysis (Quantachrome or Micromeritics instrument).

**Table 1: Specific surface area measurements by BET instrument from Micromeritics (ASPA, 2010) on TiO<sub>2</sub> NM-105, SiO<sub>2</sub> NM-200, ZnO NM-110, ZnO NM-111 and MWCNT NM-402.**

Type of materials	Former NM code	BET surface m <sup>2</sup> /g	BET surface JRC m <sup>2</sup> /g
TiO <sub>2</sub>	NM-105	32.85	46.18
SiO <sub>2</sub>	NM-200	165.21	189.16
ZnO naked	NM-110	9.79	12.4
ZnO coated	NM-111	8.09	15.1
MWCNT	NM-402 (990244)	217.84	226.39
MWCNT	NM-402 (990700)	244.47	

**Table 2: Total and micropore volume were evaluated by BET instrument from Micromeritics (ASAP, 2010) of TiO<sub>2</sub> NM-105, SiO<sub>2</sub> NM-200, ZnO NM-110, ZnO NM-111 and MWCNT NM-402.**

Type of material	Former ENMS code	Total pore volume cm <sup>3</sup> /g	Total pore volume JRC cm <sup>3</sup> /g	Micropore volume cm <sup>3</sup> /g	Micropore volume JRC cm <sup>3</sup> /g
TiO <sub>2</sub>	NM-105	0.060692	0.1937	0.011955	0.0
SiO <sub>2</sub>	NM-200	0.961186	0.7905	0.007768	0.01181
ZnO naked	NM-110	0.022180	/*	0.000741	0.000805
ZnO coated	NM-111	0.012652	/*	0.004076	0
MWCNT	NM-402 (990244)	0.5601	0.8892	0.00876	0.00814
MWCNT	NM-402 (990700)	0.156458		0.039186	

\* These values were not reported.

### **2.1.2 X-ray photoelectron spectroscopy (XPS) measurements**

XPS analysis was performed to identify chemical elements present at the extreme surface of ENMs powder samples (

**Table 3).** This technique gives information on the material elemental surface composition (depth of about 10 nm). Powders were spread on top of a double-face adhesive carbon tape, and the measurements were performed on a K-alpha spectrometer using monochromatised X-ray Al K $\alpha$  X-rays ( $h\nu = 1486.6$  eV).

TiO<sub>2</sub> ENMs results demonstrated they were less pure compared to the JRC values. The only surface contaminant detected was hydrocarbon. Trace contaminant, such as: chloride was detected and may come from the reactants used during industrial synthesis (ex: TiCl<sub>4</sub>).

SiO<sub>2</sub> ENMs contains hydrocarbon contamination, which is attributed to adsorbed carbon on the surface. In addition, Na was detected as an impurity on the final product, probably because SiO<sub>2</sub> NM-200 has been synthesised by a precipitation process where Na<sub>2</sub>SO<sub>4</sub> compound is involved.<sup>5</sup>

ZnO ENMs results are extremely different from the JRC data (atomic percentages). A percentage higher than 35 % of Zn is observed in both samples (uncoated and coated) while JRC reported values lower than 10%. We supposed that our powder samples had lower coverage compared to the JRC ones. In their case, there was a signal detected from the tape and from the powder itself. In both NM-110 and NM-111 samples, hydrocarbon contamination and Si elements are observed. For NM-111, this result is expected, given that this powder was coated with triethoxycapryl silane and hence the Si signal contribution appeared. However, this result is surprising for NM-110, which is uncoated and therefore doesn't contain any Si. The observation of Si in NM-110 could be due to contamination coming from SiO<sub>2</sub> NM-200 powder which was analysed at the same time (same sample holder). From the JRC samples, we observed clearly a low % of Si (0.3 %) for NM-110 (< 1 at% is attributed to Si presence in the adhesive tape) and a higher percentage (3.5%) for NM-111, which may relate to the coating molecule.

Besides the expected presence of C and O in MWCNT, Al impurity was detected. This can be attributed to the fact that inorganic catalysts were used in the industrial synthesis of MWCNT. Even if heterogeneous catalysis was employed, traces of some metallic elements (ex: Al, Fe, Cu, Si...) may remain. Results cannot be compared to the JRC ones, as they have evaluated the elemental composition of MWCNT with the Energy dispersive X-ray spectroscopy (EDS) technique. In addition, the results are given in wt % and mass-based parts per million (ppm).

**Table 3: Elemental chemical composition by XPS measurements on TiO<sub>2</sub> NM-105, SiO<sub>2</sub> NM-200, ZnO NM-110, ZnO NM-111 and MWCNT NM-402.**

Material	Former NM code	Surface chemical composition (at%)	Surface chemical composition JRC (at%)
TiO <sub>2</sub>	NM-105	Ti (28.48), O (58.81), C (11.98), Cl (0.74)	Ti (21.5 ± 0.4), O (54.0 ± 0.3), C (24.5 ± 0.6)
SiO <sub>2</sub>	NM-200	Si (37.42), O (60.05), C (2.08), Na (0.45)	Si (24.1 ± 0.5), O (70.8 ± 0.6), C (4.1 ± 0.9), Na (1 ± 0.2), S (0.06 ± 0.04)
ZnO naked	NM-110	Zn (38.46), O (46.54), C (10.60), Si (4.40)	Zn (5.6), O (25.1), C (69.0), Si (0.3)
ZnO coated	NM-111	Zn (43.82), O (43.25), C (9.26), Si (3.66)	Zn (4.3), O (24.3), C (67.9), Si (3.5)
MWCNT	NM-402 (990244)	C (98.56), O (0.86), Al (0.58)	/
MWCNT	NM-402 (990700)	C (98.77), O (1.23)	/

### 2.1.3 Transmission Electron Microscopy (TEM) measurements

TEM was used to identify shape, morphology and particle size (agglomeration state) of ENMs in dry state. The NanoGENOTOX dispersion protocol and the SOP for calibration of Probe-sonicators for *in vitro* and *in vivo* testing were used for the suspension's preparation. A stock solution of 2.56 mg/mL in water only was prepared and sonicated for 15 min using Branson probe-sonicator (450D, 300Watt, 10%Ampl, 13 mm horn). A suspension of 0.1 mg/mL in Elendt M7 medium (preparation medium is based on OECD TG-211 (2012), OECD TG-202 (2004) and Elendt (1990), with minor modifications in methodology for practical reasons) was prepared from the stock solution and was analysed using a TEM Instrument (Tecnai 10 Philips operating at 80 k). A droplet was deposited on a carbon-coated copper grid.

TiO<sub>2</sub> NM-105 (**Figure 1**) appear as large nanoclusters composed of primary particles linked by weak chemical bonds (agglomerates). They have some spherical and ellipsoidal structures. The primary particles have a diameter in the range from about 10 nm to 40 nm as described

in the JRC report. We cannot determine with accuracy the primary particle size due to agglomeration. The referenced value is between 15-24 nm.

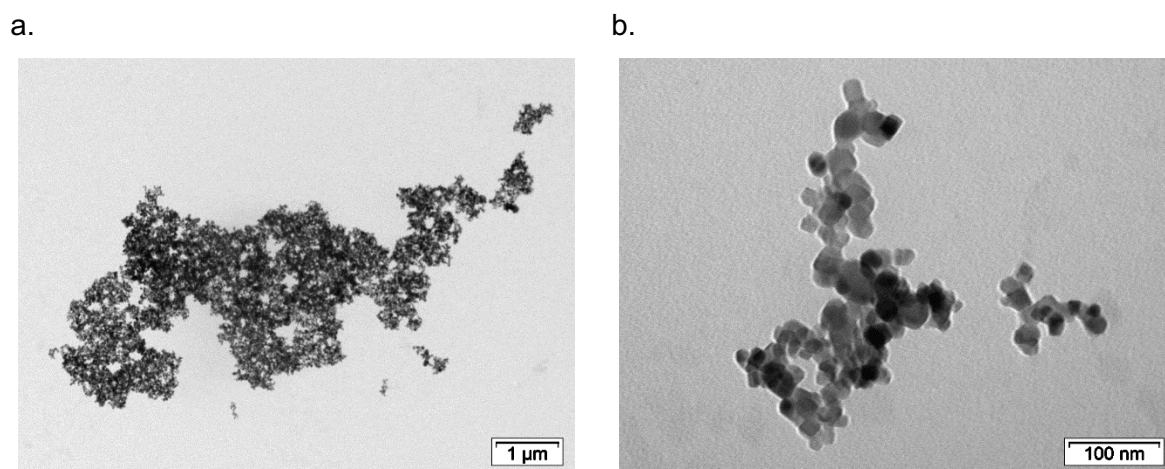


**Figure 1: TEM images of TiO<sub>2</sub> NM-105 in Elendt M7 (0.1 mg/mL) recorded at a magnification of a. 1 μm, b. 100 nm.**

SiO<sub>2</sub> NM-200 (**Figure 2**) shows a different behaviour compared to TiO<sub>2</sub> NM-105. Particles are not only agglomerates, most of them are aggregated (strong chemical bonds between ENMs), and the shape tends to be ellipsoidal. Due to this aggregation phenomenon, the diameter of the primary particles cannot be calculated. The nominal size referenced is between 14-23 nm.

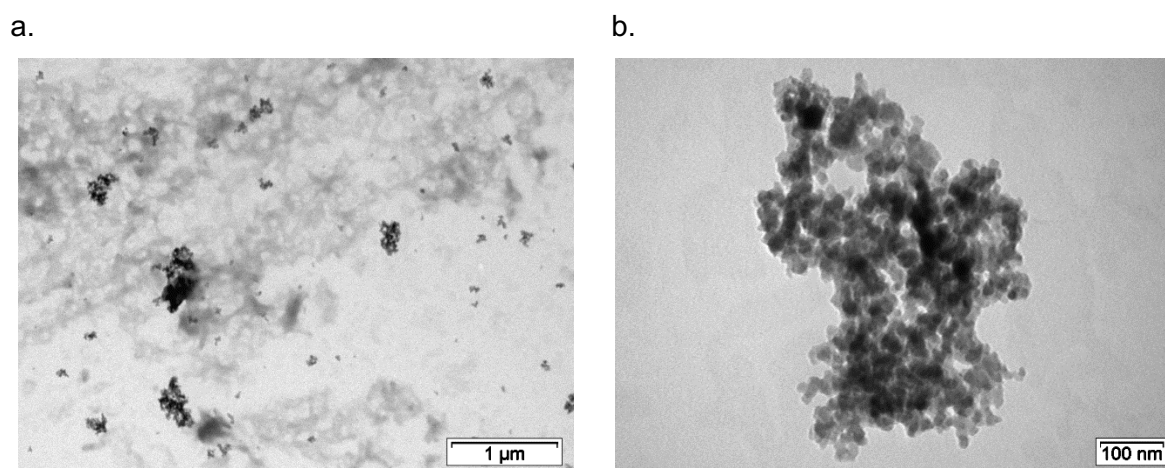


**Figure 2: TEM images of SiO<sub>2</sub> NM-200 in Elendt M7 (0.1 mg/mL) recorded at a magnification of a. 1 μm, b. 100 nm**

ZnO NM-110 (**Figure 3**) appear as large agglomerates and seem to be polyhedral. Different kind of shapes are observed as rods, spheres, cubes and hexagons. Particle size distribution ranges from 30 to 200 nm. The longest rod-shaped particles tend to have a length near 200

nm, the cubic shaped ones have a length near 100 nm, while the spherical structures have a diameter below 50 nm. Particle size distributions are as expected, and are comparable to the ones from the JRC report. The nominal size referenced is 158 nm.

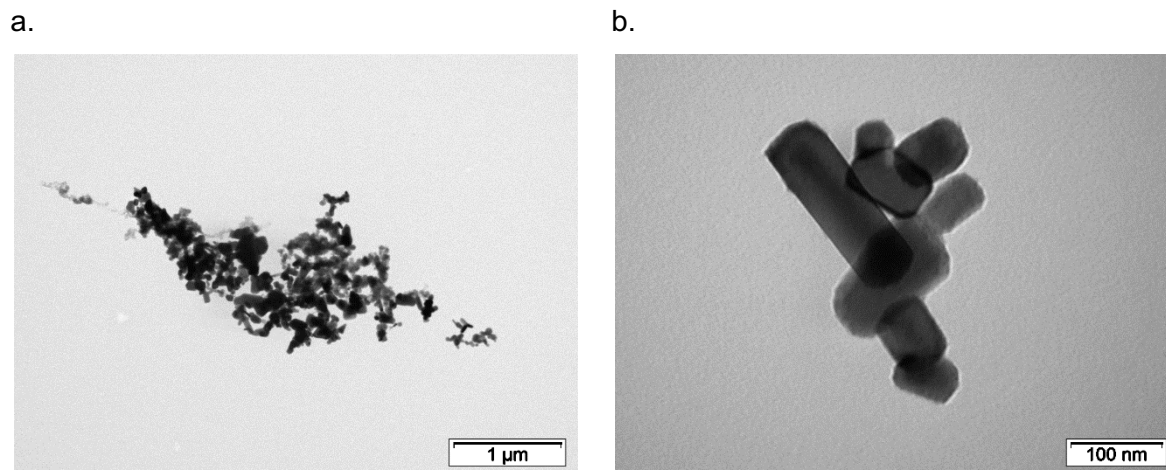


**Figure 3: TEM images of ZnO naked NM-110 in Elendt M7 (0.1 mg/mL) recorded at a magnification of a. 1 μm, b. 100 nm**

TEM images of ZnO NM-111 (**Figure 4**) are very similar to ZnO NM-110. The same kind of shapes and particle size distributions are observed. For this sample, JRC reports several different size distributions<sup>7</sup>; particles with an aspect ratio 2 to 8.5, ranging from 10 to 450 nm and the nominal size referenced is 152 nm. When compared to ZnO NM-110, there are many more particles on top of each other, and the aggregation seems prevalent. This behaviour is not expected. The presence of a coating should generate more individual ENMs while favouring deagglomeration.

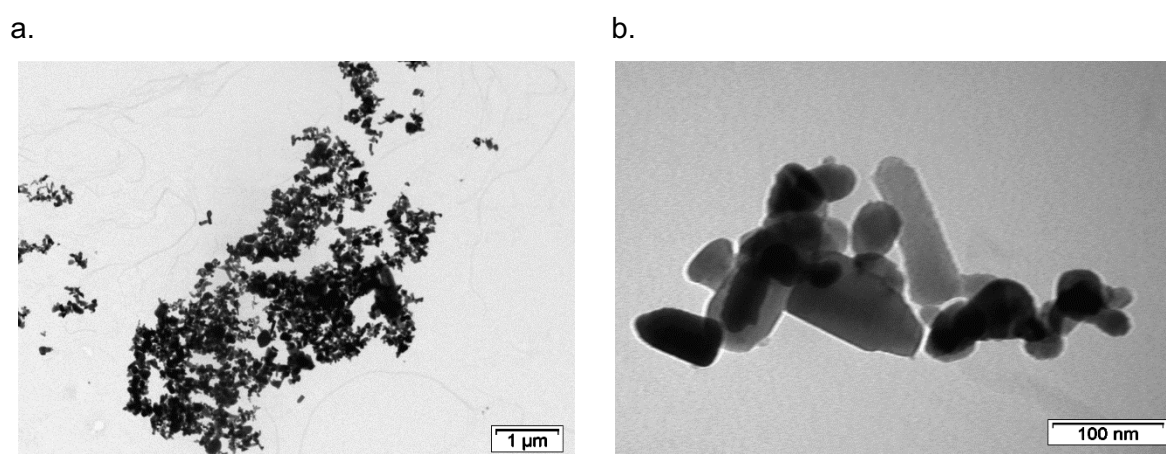
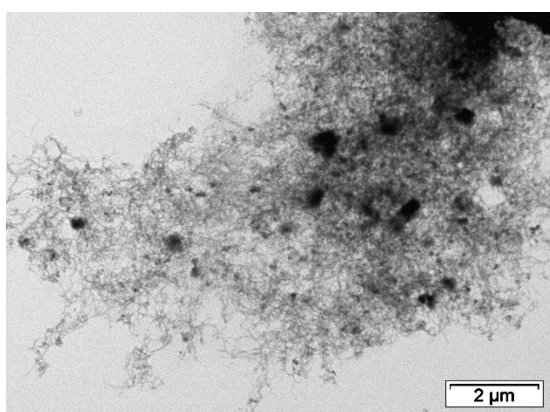


**Figure 4: TEM images of ZnO coated NM-111 in Elendt M7 (0.1 mg/mL) recorded at a magnification of a. 1 μm, b. 100 nm.**

It should be noted that MWCNT NM-402 (**Figure 5**) are neither soluble in water nor in M7 medium. Dispersing MWCNT remains a challenge. Therefore, it is not surprising to observe a high density of entangled MWCNT in the resultant images. This entanglement complicates the tube length determination. JRC reports a particle size distribution between 400 nm and 4.05  $\mu\text{m}$  and an average length of 1372 nm. These parameters depend on the type of MWCNT, the dispersion protocol used and the type of synthesis.<sup>6</sup> However, thickness has been calculated and the large majority of MWCNTs had a thickness of 11 nm. These results are in good agreement with JRC and Coda-Cerva laboratory data.

a.



b.

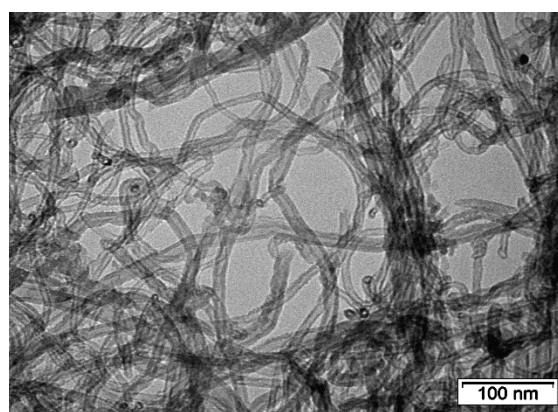


**Figure 5: TEM images of MWCNT NM-402 in Elendt M7 (0.1 mg/mL) recorded at a magnification of a. 2  $\mu\text{m}$ , b. 100 nm.**

#### 2.1.4 Effective density measurements

ENMs mass transport mechanisms, such as sedimentation and/or diffusion processes, is greatly affected by the formation of agglomerates in suspension. These are composed of several primary ENMs particles around which media is entrapped. The density of the dispersing media is lower compared to the density of primary ENMs particles. Therefore, the density of an agglomerate is lower compared to the density of a primary particle<sup>5-9</sup>. Effective density determination is an important step to understand ENMs mass transport properties in dosimetry studies.

The technique used for this purpose is the volumetric centrifugation method (VCM). Effective density ( $\rho_{EV}$ ) was calculated by using the equation below which contains parameters including the density of the medium ( $\rho_{media}$ ), initial mass of ENMs ( $M_{ENM}$ ), solubilised mass of ENMs ( $M_{ENSol}$ ) and stacking factor ( $SF$ ). A SF of 0.634 was used in calculations and considers roughly spherical agglomerates of ENMs.

$$\rho_{EV} = \rho_{media} = \left[ \left( \frac{M_{ENM} - M_{ENSol}}{V_{pellet} \times SF} \right) \times \left( 1 - \frac{\rho_{media}}{\rho_{ENM}} \right) \right]$$

The NanoGENOTOX dispersion protocol and the SOP for calibration of Probe-sonicators for *in vitro* and *in vivo* testing were used for the suspension's preparation. A stock solution of 1.28 mg/mL in water was prepared and was sonicated for 15.4 min using a Branson Sonifier S-450D (Branson Ultrasonics, 300Watt, 10%Ampl, 13 mm horn). A volume of 1 mL stock solution was added to PCV tubes. The experiment was performed 6 times (6 samples). Tubes were centrifuged (Centrifuge 5702, Eppendorf) for 30 min at 4400 rpm to obtain a pellet in the bottom. The volume of the pellet ( $V_{\text{pellet}}$ ) was measured using a slide rule-like easy-measure device ("Easy read" measuring device TPP). Supernatants of three PCV tubes were collected after centrifugation. They were mixed together, and a solution of aqua regia (25% aqua regia: 75% sample) is added to mineralise the sample and transform nanoparticles in ions. Samples were analysed by Inductively Coupled Plasma - Optical Emission Spectrometry (ICPO-OES) to determine the mass of suspended ENMs. In the case of ZnO ENMs, pH of the suspensions was modified to prevent the powder from sticking to the tube walls after centrifugation. An alkaline solution (100 uL of NaOH) was added in each PCV tubes. The same procedure was conducted for MWCNT NM-402 suspended in water but the centrifugation was not efficient neither for the batch 990244 nor for 990700. For this reason, effective density cannot be calculated for MWCNT.

Results are described in

**Table 4.** Deloid et *al.*<sup>8</sup> have performed the same experiment and they have obtained an effective density of  $1.315 \pm 0.007$  for  $\text{TiO}_2$  (Evonik),  $1.112 \pm 0.001$  for  $\text{SiO}_2$  (Venges) and  $1.650 \pm 0.07$  for ZnO (Alfa Aesar). Our results are not comparable to theirs. ENMs suppliers are different, and their experiment was performed in cell culture media (proteins may have a protein corona around primary ENMs particles and may affect the agglomerate density).

**Table 4 : Raw ENMs materials density ( $\rho_{ENM}$ ) and effective density ( $\rho_{EV}$ ) estimated in our laboratory by volumetric centrifugation in water of TiO<sub>2</sub> NM-105, SiO<sub>2</sub> NM-200, ZnO NM-110 and NM-111. Errors were calculated based on the standard deviation (s.d) on six measurements.**

Materials	Former NM code	$M_{ENsol}$ %	$\rho_{ENM}$ (g/cm <sup>3</sup> )	$\rho_{EV}$ (g/cm <sup>3</sup> )
TiO <sub>2</sub>	NM-105	0.394	4.230	1.422 ± 0.013
SiO <sub>2</sub>	NM-200	3.638	2.648	1.349 ± 0.016
ZnO naked	NM-110	2.038	5.606	2.225 ± 0.037
ZnO coated	NM-111	2.044	5.606	2.202 ± 0.036

## 2.2 Evaluation of the ecotox testing water column

ISTEC was responsible for characterising the colloidal behaviour of ENM by quantifying their concentration in the ecotox testing water column, with the use of the spectroscopic method, ICP-OES.

### 2.2.1 Experimental part

#### 2.2.1.1 Materials.

Titanium dioxide, NM-105, and Zinc oxide, NM-110 and NM-111, were provided as nano-powders by JRC in Ispra (Italy). Cerium dioxide, NM-212, was purchased from Fraunhofer-Gesellschaft (Germany). The dissolved ionic Ce, Ti and Zn standard for ICP-OES, hydrogen peroxide solution (95321) and nitric acid (84380-M) were purchased from Sigma-Aldrich (St. Louis, MO, US). All the Elendt M7 medium salts were purchased from Sigma-Aldrich, Milan (Italy); their approximate composition in mg L<sup>-1</sup> is 0.715 H<sub>3</sub>BO<sub>3</sub>, 0.090 MnCl<sub>2</sub>\*4H<sub>2</sub>O, 0.078 LiCl, 0.018 RbCl, 0.040 SrCl<sub>2</sub>\*6H<sub>2</sub>O, 0.004 NaBr, 0.017 Na<sub>2</sub>MoO<sub>4</sub>\*2H<sub>2</sub>O, 0.005 CuCl<sub>2</sub>\*2H<sub>2</sub>O, 0.015 ZnCl<sub>2</sub>, 0.012 CoCl<sub>2</sub>\*2H<sub>2</sub>O, 0.004 KI, 0.003 Na<sub>2</sub>SeO<sub>3</sub>, 0.001 NH<sub>4</sub>VO<sub>3</sub>, 1.250 Na<sub>2</sub>EDTA\*2H<sub>2</sub>O, 0.498 FeSO<sub>4</sub>\*7H<sub>2</sub>O, 293.800 CaCl<sub>2</sub>\*2H<sub>2</sub>O, 123.300 MgSO<sub>4</sub>\*7H<sub>2</sub>O, 5.800 KCl, 64.800 NaHCO<sub>3</sub>, 10.000 Na<sub>2</sub>SiO<sub>3</sub>\*9H<sub>2</sub>O, 0.274 NaNO<sub>3</sub>, 0.143 KH<sub>2</sub>PO<sub>4</sub>, 0.184 K<sub>2</sub>HPO<sub>4</sub>.

#### 2.2.1.2 Sample preparation.

Samples were prepared starting from stocks at 2.56 mg mL<sup>-1</sup> in MilliQ water + EDTA, prepared according to the NANoREG dispersion protocol. We used EDTA instead of NOM, for improving

NPs dispersibility, because it was a component of the medium and performed well. The stocks were diluted in Elendt M7 or Egg Water medium, reaching the desired concentration in the concentration range of  $0.25 - 100 \mu\text{g mL}^{-1}$ , exposing samples at  $22^\circ\text{C}$  for 1h and 72h of incubation, thus mimicking long-term exposure conditions.

### 2.2.1.3 Colloidal characterisation.

Hydrodynamic size distribution and Zeta potential (ZP -  $\zeta\text{-pot}_{\text{ELS}}$ ) measurements of the nano-suspensions were carried out with a DLS / ELS (dynamic light scattering and electrophoretic light scattering Zetasizer Nano instrument ZSP, ZEN5600, Malvern Instruments, UK) both in MilliQ water and in Elendt M7 or Egg Water medium. Titrations of ZP vs pH were also performed with automatic titration, using 1M KOH and 1M HCl to change the pH, so providing an indication on the isoelectric point (IEP) that corresponds to the pH value where ZP is neutralised.

### 2.2.1.4 Sedimentation study.

The concentration at half height of the water-column was estimated, following the set-up described in **Figure 6**. We incubated NPs in water media (15 mL falcon), collecting 3 mL of sample from the center of the water-column (9 mL). The collected 3 mL of sample were then acid digested and analysed by ICP-OES (ICP-OES 5100 – vertical dual view apparatus, Agilent Technologies, Santa Clara, CA, USA).

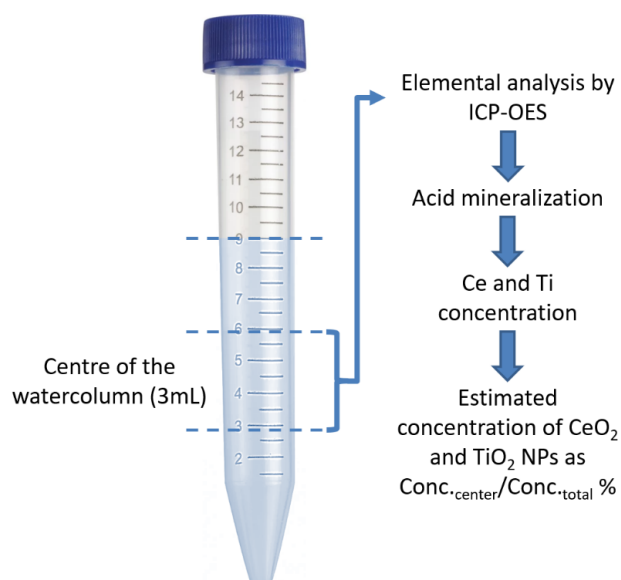


**Figure 6: Experimental set-up for the measurement of the NPs concentration at half height of water column.**

### **2.2.1.5 Analytic measurements.**

The nominal concentration of NMs in relevant medium was evaluated by inductively coupled plasma optical emission spectrometry using an ICP-OES 5100 – vertical dual view apparatus coupled with OneNeb nebuliser (Agilent Technologies, Santa Clara, CA, USA). An acid Digestion procedure was performed adding 0.3 mL of sulfuric acid (H<sub>2</sub>SO<sub>4</sub> 96%), 0.3 mL of phosphoric acid (H<sub>3</sub>PO<sub>4</sub> 85%) and 0.3 mL of nitric acid (HNO<sub>3</sub> 65%) into 3 mL sample. The treated samples were then analysed by ICP-OES. The analysis was performed in radial viewing mode, and calibration curves were obtained with 0.01, 0.05, 0.1, 1.0, 10.0 and 50.0 µg mL<sup>-1</sup> standards, sample's medium (Elendt M7 or Egg Water) was used as the matrix and the same digestive procedure was applied to standards. The wavelengths we selected were: Ce 418.7 nm, Ti 334.9 nm and Zn 206.2 nm. The calibration curve was evaluated and showed correlation coefficient (R<sup>2</sup>) above 0.99. Results from ICP-OES were reported as the average of three independent measurements with relative standard deviation (RSD) %.

### **2.2.2 Size, Zeta pot in eco-tox media**

To define physicochemical identity in support of risk assessment, two questions should be addressed: “where NPs go” and “what NPs do”<sup>10,11</sup>. For this reason, in this study, we investigated the colloidal stability (hydrodynamic size distribution and Zeta Potential) once NPs enter into relevant eco-toxicological media, reproducing both fresh and seawater conditions. An intensive DLS campaign in eco-tox media was performed, providing information on agglomeration kinetics and on colloidal stability of the dispersed systems, focusing on ZnO (NM-110 and NM-111), TiO<sub>2</sub> (NM-105) and CeO<sub>2</sub> (NM-212) NMs. To mimic long-term exposure conditions, we diluted NMs in Elendt M7, for the freshwater environment, and in Egg Water medium, for seawater environment, reaching the concentration range of 0.25 – 100 µg mL<sup>-1</sup> and exposing samples at 22°C for 1h and 72h of incubation.

#### **2.2.2.1 Zinc oxide colloidal stability**

In the Tables below we report DLS diameter and ZP of samples in a range of concentrations from 100 to 0.25 mg L<sup>-1</sup>, after 1 and 72h of exposure in Elendt M7, mimicking long term exposure conditions (**Table 5** and **Table 6**). At all investigated concentrations and times of exposure, we observe a high agglomeration degree with the formation of micro-aggregates, even at low concentrations, despite ZP values of > -15 mV which should provide an electrostatic stabilisation. For NM-110 NPs after 72h of incubation for all concentrations, an increase in size distribution occurs as well as an increase of polydispersity index (PDI). The NM-110 NPs in Elendt M7 tend to aggregate and precipitate along the water-column as a

function of time. However, this colloidal behaviour is not confirmed for NM-111 NPs across all concentrations, but only above 10 mg L<sup>-1</sup>. Below 5 mg L<sup>-1</sup>, this trend is inversed and NM-111 NPs seem to be more dispersed after 72h of exposure, where we observed a reduction in size distribution and PDI. Below 10 mg L<sup>-1</sup> we have a nearly constant value for both NPs types (ca. -18 mV). The ZP values change from positive to negative, passing through the stock dispersion value (positively charged) to the samples diluted in Elendt M7 (negatively charged), probably due to specific adsorption on NPs surfaces of anionic salts that are present in Elendt M7, such as phosphate<sup>12,13</sup>.

**Table 5 : DLS and ELS measurements for NM-110 in Elendt M7.**

Concentration (mg L <sup>-1</sup> )	Incubation time (h)	d <sub>DLS</sub> (nm) (rsd %)	PDI (rsd %)	ζ-pot <sub>ELS</sub> (mV) (rsd %)
100	1	3224 (1284)	0.610 (0.090)	-7.1 (0.2)
	72	4105 (1493)	0.580 (0.190)	-7.9 (0.6)
50	1	3333 (394)	0.400 (0.060)	-7.9 (0.5)
	72	3392 (703)	0.400 (0.070)	-7.4 (0.6)
10	1	813 (64)	0.570 (0.070)	-18.2 (0.6)
	72	2052 (324)	0.850 (0.150)	-17.9 (0.1)
5	1	1012 (130)	0.690 (0.100)	-18.0 (0.3)
	72	2477 (391)	0.900 (0.090)	-18.2 (0.4)
2.5	1	1466 (150)	0.770 (0.120)	-19.8 (0.8)
	72	2073 (885)	0.800 (0.140)	-19.4 (0.9)
0.25	1	2614 (319)	0.360 (0.180)	-19.2 (0.4)
	72	2676 (509)	0.690 (0.210)	-17.5 (0.3)

**Table 6 : DLS and ELS measurements for NM-111 in Elendt M7.**

Concentration (mg L <sup>-1</sup> )	Incubation time (h)	d <sub>DLS</sub> (nm) (rsd %)	PDI (rsd %)	ζ-pot <sub>ELS</sub> (mV) (rsd %)
100	1	3780 (1364)	0.820 (0.240)	-10.7 (1.1)
	72	3784 (2275)	0.760 (0.260)	-17.1 (1.0)
50	1	2088 (336)	0.840 (0.180)	-9.5 (0.7)
	72	3624 (1643)	0.980 (0.040)	-12.9 (0.6)
10	1	1576 (173)	0.580 (0.160)	-17.7 (0.6)
	72	2306 (332)	0.730 (0.170)	-17.1 (0.3)
5	1	1732 (571)	0.760 (0.210)	-19.4 (0.4)
	72	816 (78)	0.510 (0.090)	-17.7 (0.5)
2.5	1	825 (103)	0.610 (0.150)	-18.9 (1.1)
	72	591 (50)	0.520 (0.040)	-17.7 (0.5)
0.25	1	2486 (685)	0.520 (0.340)	-19.2 (0.3)
	72	2448 (330)	0.300 (0.210)	-20.2 (0.5)

As in the case of ZnO samples dispersed in Elendt M7, samples dispersed in Egg Water show high instability, polydispersity and aggregation at all concentrations and incubation times (**Table 7** and **Table 8**). Micro-macro metric aggregates are detected and tend to flocculate and drop down in few minutes. In general, ZnO NPs results indicate the material is quite unstable in saline environmental media, dropping down and precipitating at the bottom of the experimental flask.

**Table 7 : DLS and ELS measurements for ZnO NM-110 in Egg Water.**

Concentration (mg L <sup>-1</sup> )	Exposure time (h)	d <sub>DLS</sub> (nm)	St. Dev.	Pdl
5.00	1	962	145	0.640
	24	2331	712	0.960
2.50	1	3368	1790	0.940
	24	3885	1675	0.930
0.25	1	5281	1759	0.870
	24	5063	3498	0.770

**Table 8: DLS and ELS measurements for ZnO NM-111 in Egg Water.**

Concentration (mg L <sup>-1</sup> )	Exposure time (h)	d <sub>DLS</sub> (nm)	St. Dev.	Pdl
5.00	1	2956	1648	0.960
	24	3750	1789	0.780
2.50	1	4958	3442	0.770
	24	3773	1564	0.690
0.25	1	5470	4441	0.800
	24	3734	1141	0.590

To better understand the pH effect on colloidal stability, we considered samples dispersed in water and Elendt M7 for 1h and performed ZP titration as a function of pH. We measured and compared the isoelectric point (IEPs), the pH where ZP is neutralized<sup>14</sup>, of naked (**Figure 7**) and coated NPs (**Figure 8**) in MilliQ water and Elendt M7. This generated information on NPs surface chemistry, that, after exposure, can become more acid (shift of IEP towards lower pH) or more basic (shift of IEP to higher pH). When examining the ZP vs pH curves in water, the presence of two IEPs marked with red arrows in the Figures 7 and 9 can be observed. This behaviour is typical of surfaces that have undergone a strong modification induced by a pH change, such as for instance the dissolution phenomena. In the case of ZnO NPs we make the hypothesis that, immediately after immersion, the ZnO NPs surface is hydrolysed with the formation of a Zn(OH)<sub>2(s)</sub> layer. As pH decreases (pH<6)<sup>15</sup> the surface partially solubilises, releasing Zn<sup>2+</sup> and Zn(OH)<sup>+</sup> ions, which could re-precipitate resulting in a new solid phase ZnOx<sub>(s)</sub>, that shows a new IEP at low pH<sup>15,16</sup>, together with a reduced hydrodynamic size (**Figure** ).

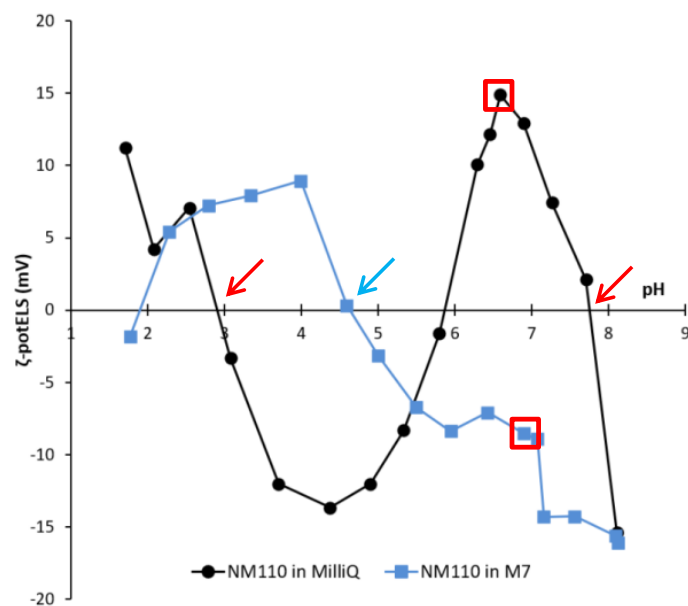


**Figure 7: Zeta Potential (mV) vs pH plot of ZnO NM-110 MilliQ (●) and Elendt M7 (■) media (nanosol; □ natural pH, IEPs red arrow for MilliQ (→) and blue arrow for Elendt M7(→)).**

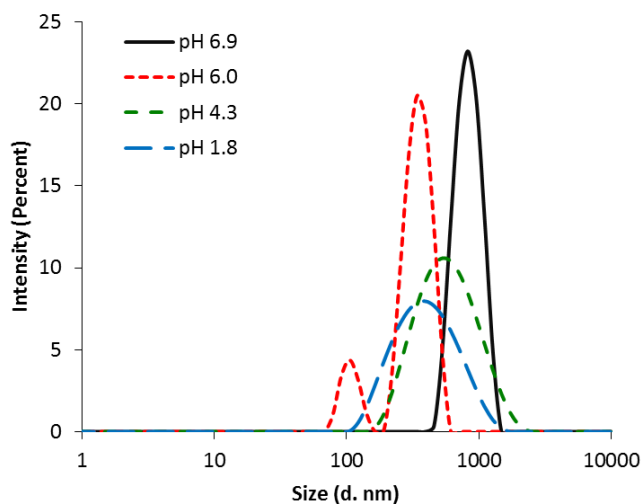


**Figure 8 : Size distribution of ZnO NM-110 MilliQ medium at different pH (- 6.9, - 6.0, - 4.3, - 1.8).**

The same behaviour was also observed with ZnO NM-111 NPs, where the ZP positive values lie between pH 6.3 and 7.5 in distilled water and shifts in Elendt M7 medium to a pH lower than 2.7 for the presence of co-exposed anions ( $\text{SO}_4^{2-}$ ,  $\text{PO}_4^{3-}$ ). The coating presence change the electrophoretic mobility change, shifting and reducing the ZP positive values range and both IEPs.

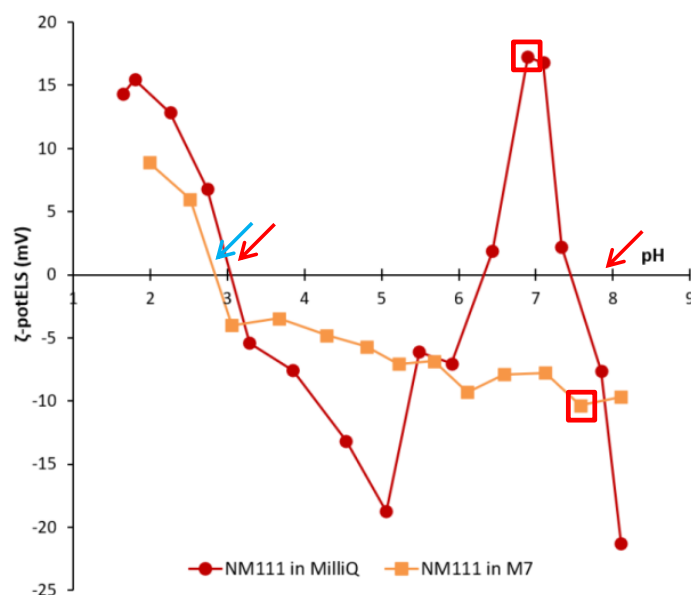


**Figure 9: Zeta Potential (mV) vs pH plot of ZnO NM-111 MilliQ (●) and Elendt M7 (■) media; □ natural pH, IEPs red arrow for MilliQ (→) and blue arrow for Elendt M7(→)).**

The ELS results show a high instability of water suspensions for both ZnO NPs type. Both NPs present a fluctuation of ZP values between 20 mV and -20 mV once dispersed in water ( $1 < \text{pH} < 9$ ), presenting a high colloidal instability<sup>16</sup>. Thus, the size dimension observed in the DLS analysis (**Table 7** and **Table 8**) confirmed this high instability and agglomeration trend, providing the micro-aggregates formation. Since instability was confirmed in water medium, different behaviour was observed in Elendt M7, where both ZnO NPs present a slightly negative superficial charge. At pH 7 in Elendt M7, ZP values are close to -10 mV, so from water to ecotox medium the ZP values change from positive (15 mV) to negative, probably due to salt amounts within the medium.

### **2.2.2.2 Titanium dioxide colloidal stability**

As for ZnO NPs, we proceeded with the characterisation of system-dependent colloidal properties evaluation, considering freshwater and seawater exposure conditions. In particular, we focused on the possible scenario of  $\text{TiO}_2$ , both in Elendt M7 and Egg water.

### **2.2.2.3 $\text{TiO}_2$ in Elendt M7**

The colloidal stability of  $\text{TiO}_2$  NPs was further evaluated by measuring the hydrodynamic size ( $d_{\text{DLS}}$ ) of samples dispersed in Elendt M7 medium at low concentration, mimicking exposure conditions of *Daphnia magna*<sup>17,18,19</sup> (0.02, 0.20, 2.00 and 5.00 mg L<sup>-1</sup>). As reported in **Table 9**,

all samples present a strong degree of agglomeration, more evident at low concentrations; the size distribution passing from ca. 800 nm for the 5 mg L<sup>-1</sup> sample to ca. 3000 nm for the 0.02 mg L<sup>-1</sup> sample. No appreciable differences are observable in time and size distribution values remain almost constant from 1h to 24h of exposure. So, the main change occurs in the first hour of exposure. TiO<sub>2</sub> NPs once dispersed in Elendt M7 agglomerated in almost micro-aggregates with high polydispersity (PDI > 0.600).

**Table 9: DLS measurements of TiO<sub>2</sub> in Elendt M7 medium.**

Sample concentration (mg L <sup>-1</sup> )	d <sub>DLS</sub> distribution (nm) after an exposure time		
	1h	2h	24h
<b>0.02</b>	2457 ± 832 (PDI: 0.600 ± 0.300)	3268 ± 1230 (PDI: 0.670 ± 0.300)	2495 ± 552 (PDI: 0.720 ± 0.300)
<b>0.2</b>	1701 ± 515 (PDI: 0.740 ± 0.210)	2350 ± 758 (PDI: 0.770 ± 0.250)	2004 ± 633 (PDI: 0.850 ± 0.200)
<b>2.0</b>	906 ± 401 (PDI: 0.700 ± 0.160)	960 ± 597 (PDI: 0.700 ± 0.150)	1267 ± 681 (PDI: 0.760 ± 0.160)
<b>5.0</b>	882 ± 480 (PDI: 0.650 ± 0.190)	628 ± 172 (PDI: 0.590 ± 0.140)	899 ± 237 (PDI: 0.660 ± 0.130)

ZP curve as a function of pH is reported in [Error! Reference source not found.](#) TiO<sub>2</sub> NPs present the typical amphiphilic behaviour of oxide NPs dispersed in water, positive at acid pH and negative for a basic environment, showing, in agreement with literature, the IEP at pH 6.5<sup>1,21,22</sup>. Once dispersed in Elendt M7 medium, TiO<sub>2</sub> NPs show a slight shift of IEP (pH 5.4)<sup>15,16</sup>, most likely due to the adsorption of co-exposed anions (SO<sub>4</sub><sup>2-</sup>, PO<sub>4</sub><sup>3-</sup>) at the NPs surface. In addition, the ZP values are flattened and lowered with values between 20 mV and -10 mV, due to the presence of indifferent ions (Cl<sup>-</sup>, Br<sup>-</sup>, I<sup>-</sup>, NO<sub>3</sub><sup>-</sup>), that reduce the double layer thickness at the NPs surface.

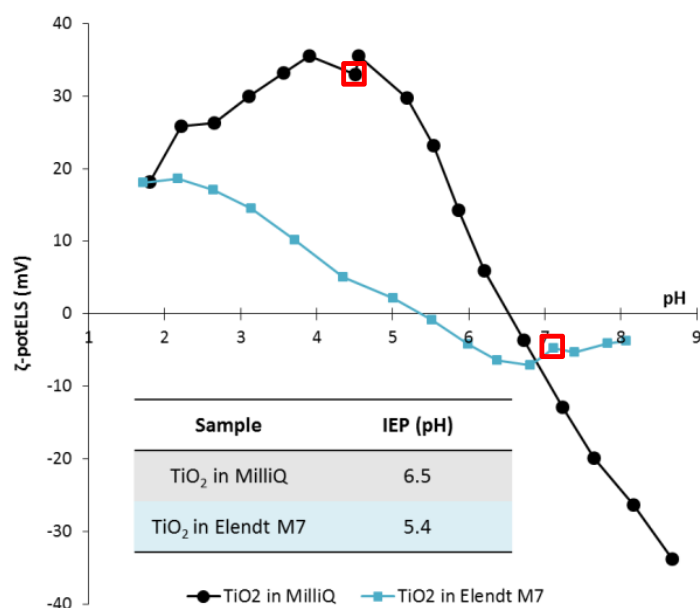


**Figure 10 : Zeta Potential (mV) vs pH plot of TiO<sub>2</sub> in MilliQ (●) and in Elendt M7 (■) media (nanosol concentration 100 mg L<sup>-1</sup> - ■ natural pH).**

#### **2.2.2.4 TiO<sub>2</sub> in Egg Water**

As for Elendt M7, the colloidal stability of TiO<sub>2</sub> NPs was further evaluated by measuring the hydrodynamic size ( $d_{DLS}$ ) of samples dispersed in Egg water medium at a low concentration, mimicking exposure conditions of Zebrafish<sup>25,26,27</sup> (2.0, 5.0 and 10.0 mg L<sup>-1</sup>). In this case, we selected a higher concentration range to identify the concentration limit, above which the system is strongly affected by the time of exposure. What we found is that at all concentrations, samples present a high instability with a time dependent increase of hydrodynamic diameter from about 800 nm (after 1h) to about 3000 nm (after 24h) for all concentrations tested (**Table 10**).

**Table 10 : DLS measurements of TiO<sub>2</sub> in Egg Water medium.**

Sample concentration (mg L <sup>-1</sup> )	$d_{DLS}$ distribution (nm) after an exposure time		
	1h	2h	24h
<b>2.0</b>	746 ± 299 (PDI: 0.590 ± 0.160)	1171 ± 283 (PDI: 0.410 ± 0.210)	3392 ± 1037 (PDI: 0.960 ± 0.120)
<b>5.0</b>	846 ± 230 (PDI: 0.610 ± 0.170)	1401 ± 221 (PDI: 0.460 ± 0.160)	3275 ± 2378 (PDI: 0.840 ± 0.190)
<b>10.0</b>	750 ± 103 (PDI: 0.520 ± 0.110)	1376 ± 248 (PDI: 0.350 ± 0.190)	3079 ± 1211 (PDI: 0.810 ± 0.230)

In this case, the increase in size distribution is time-dependent and does not appear to be affected by variation in concentration (from 2 to 10 mg L<sup>-1</sup>) and the main size dimension changes for all samples from ca. 800 nm after 1h to ca. 3000 nm after 24h of exposure. As in Elendt M7, TiO<sub>2</sub> NPs once dispersed tended to agglomerate in almost micro-aggregates with high polydispersity (PDI ≥ 0.600).

The ZP vs pH curve, measured in Egg water, in comparison with MilliQ water is reported in Error! Reference source not found.. Also, in this case, we noticed a slight shift of IEP towards acidic pH, even the natural ZP is higher than that measured in Elendt M7.

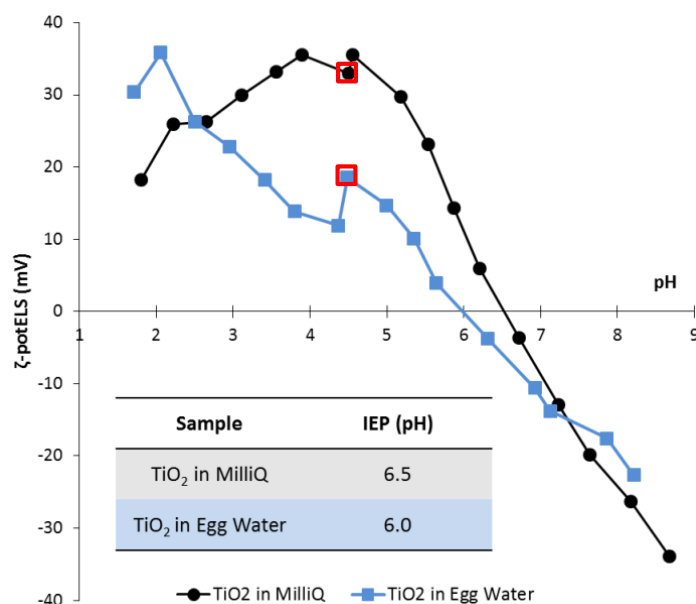


**Figure 11 : Zeta Potential (mV) vs pH plot of TiO<sub>2</sub> in MilliQ (●) and in Egg Water (■) media (nanosol concentration 100 mg L<sup>-1</sup> - ■ natural pH).**

### **2.2.2.5 Cerium dioxide colloidal stability**

The colloidal stability of CeO<sub>2</sub> NPs in Elendt M7 was evaluated by measuring the hydrodynamic  $d_{DLS}$  at the concentration of 0.02, 0.20, 2.00 and 5.00 mg L<sup>-1</sup> and 1 - 24 h of exposure. From the first hour we noticed the presence of micrometric aggregates that dramatically increased after 24h.

As for TiO<sub>2</sub>, we evaluated the change in colloidal stability of CeO<sub>2</sub> NPs in MilliQ water and in Elendt M7, to predict their behaviors in environmental medium. The curves of ZP as a function of pH are reported in Error! Reference source not found.2. In MilliQ water CeO<sub>2</sub> NPs in a similar

manner to TiO<sub>2</sub> NPs, presenting the typical amphiphilic behavior of oxide NPs dispersed in water, positive at acidic pH and negative in a basic environment, showing, in agreement with the literature, the IEP at pH 6.8<sup>28</sup>. Otherwise, CeO<sub>2</sub> NPs seem strongly affected by the medium, the IEP shifts to pH 2, as the NPs surface was totally covered by co-exposed anions (SO<sub>4</sub><sup>2-</sup>, PO<sub>4</sub><sup>3-</sup>). Furthermore, the improved ionic strength of medium overall decreases the ZP, flattening the curve around values close to 0 mV, promoting the agglomeration confirmed by the data summarised in **Table 11**.

**Table 11 : DLS measurements of CeO<sub>2</sub> in Elendt M7 medium.**

Sample concentration (mg L <sup>-1</sup> )	d <sub>DLS</sub> distribution (nm) after an exposure time		
	1h	2h	24h
0.2	2778 ± 848 (PDI: 0.570 ± 0.240)	3957 ± 1371 (PDI: 0.630 ± 0.260)	3135 ± 805 (PDI: 0.700 ± 0.260)
2.0	2264 ± 536 (PDI: 0.640 ± 0.260)	2842 ± 902 (PDI: 0.630 ± 0.250)	7401 ± 1099 (PDI: 0.790 ± 0.260)
5.0	1866 ± 412 (PDI: 0.720 ± 0.190)	2343 ± 564 (PDI: 0.400 ± 0.200)	10220 ± 1831 (PDI: 0.910 ± 0.160)

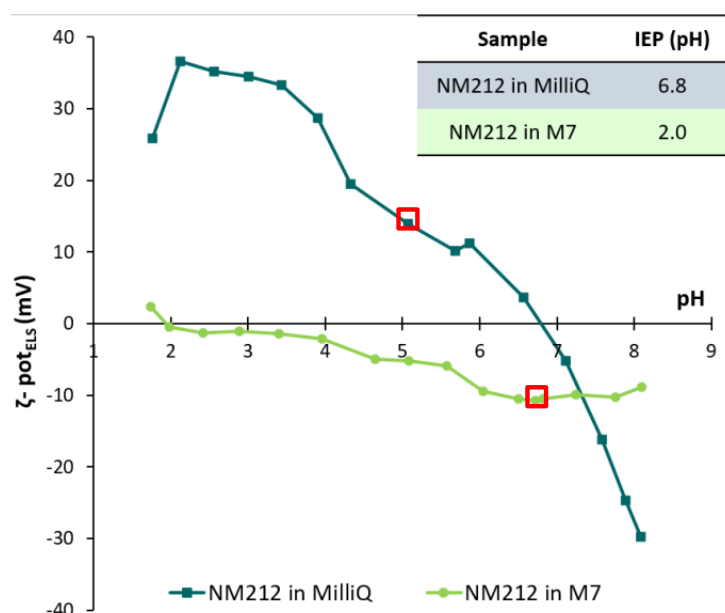


**Figure 12: Zeta Potential (mV) vs pH plot of CeO<sub>2</sub> in MilliQ (■) and in Elendt M7 (●) media (nanosol concentration 100 mg L<sup>-1</sup> - ■ natural pH).**

### 2.2.2.6 Conclusions

In this study we investigated the colloidal stability of ZnO (NM-110 and NM-111), TiO<sub>2</sub> (NM-105) and CeO<sub>2</sub> (NM-212) NMs, mimicking the exposure conditions of *in vivo* tests performed, respectively, with *Daphnia magna* and Zebrafish. Zeta potential titrations as a function of pH allowed us to estimate the surface acidity transformation that occurred (shift of IEP) when NPs are dispersed in environmental media. The hydrodynamic diameter measured at different concentrations and exposure times confirmed the high degree of agglomeration. There is a correlation between NPs agglomeration and time of exposure.

### **2.2.3 Height concentration profiles in eco-tox media**

Using the experimental set-up illustrated in **Figure 6**, we measured the NPs concentration at half height of a water column model, obtaining sedimentation curves and information about the overall colloidal stability of TiO<sub>2</sub> and CeO<sub>2</sub>, in Elendt M7 and Egg water. The aim of this study is to support the estimation of particles that come into contact with the biological target and can determine an adverse effect (dose).

#### **2.2.3.1 TiO<sub>2</sub> in Elendt M7**

The presence of salts, even though Elendt M7 is a freshwater medium, can alter the colloidal behaviour of the system while decreasing the suspension stability along the water column<sup>29,30</sup>, during the 48h of exposure. In **Table 12** and in **Figure** , we summarised the profile concentration of TiO<sub>2</sub> exposed to Elendt M7, referring to the central part of the water-column (experimental set-up reported in **Figure 6**).

**Table 12 : Half water column height concentration expressed as TiO<sub>2</sub> Conc. center / Conc. total %, after 1, 24 and 48 hours of exposure in Elendt M7.**

Concentration (mg L <sup>-1</sup> )	NPs percentage (%)		
	% 1h	% 24h	% 48h
<b>0.02</b>	75	72	68
<b>0.2</b>	85	75	73
<b>2</b>	89	73	60
<b>5</b>	94	19	8

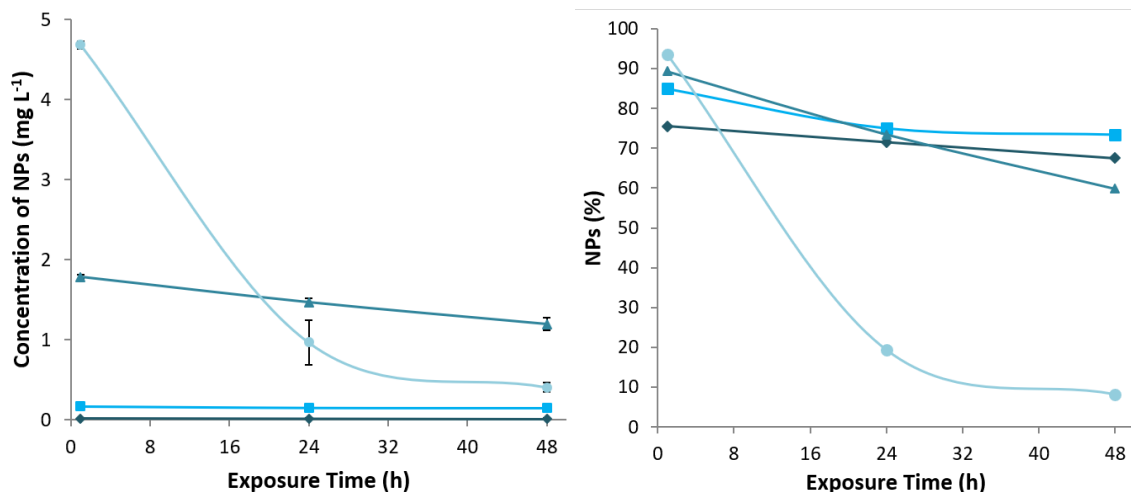


**Figure 13: (left) NPs concentration (mg L<sup>-1</sup>) and (right) NPs concentration (%) in the central part of water column for (♦) 0.02, (■) 0.2, (▲) 2 and (●) 5 mg L<sup>-1</sup> samples as a function of time (1, 24 and 48 h).**

The results show that in more concentrated samples, the progress of agglomeration and precipitation vs time of exposure occurs with higher intensity, most evident for sample at 5 mgL<sup>-1</sup>, where only 10% of the initial concentration is found after 48h. Otherwise, at low concentrations, the samples are stable, with only a slight decrease in concentration after 48h (NPs percentage in the center of ca. 60% / 70%).

### **2.2.3.2 TiO<sub>2</sub> in Egg Water**

Sedimentation curves are reported in **Table 13** and Error! Reference source not found. for TiO<sub>2</sub> exposed to Egg water medium. The results confirmed the instability observed by DLS measurements, and the measured concentrations dropped after 24h.

**Table 13 : Half water column height concentration expressed as TiO<sub>2</sub> Conc. center / Conc. total %, after 1, 24 and 48 hours of exposure in Egg water.**

Concentration (mg L <sup>-1</sup> )	NPs in the central column (mg L <sup>-1</sup> ) after:						NPs percentage (%)		
	2h	(rsd)	4h	(rsd)	24h	(rsd)	% 2h	% 4h	% 24h
<b>2.0</b>	1.79	0.03	1.72	0.04	0.88	0.08	96	92	47
<b>5.0</b>	4.29	0.09	4.23	0.07	1.57	0.17	95	94	35
<b>10.0</b>	8.85	0.09	8.38	0.13	2.66	0.49	99	94	30

Samples in Egg water were stable in the first 2h, but started to precipitate just after the first four hours of exposure, most likely due to the presence of a higher concentration of salts, as

compared to the fresh water Elendt M7 medium. After 2h of exposure, the agglomeration and precipitation processes occurred and the NPs percentage was drastically reduced in the water-column center, reaching values of ca. 37%. The agglomeration and precipitation phenomena are more evident in the 10 mg L<sup>-1</sup> sample (30%) and more attenuated in the 2 mg L<sup>-1</sup> sample (47%), as function of concentration.

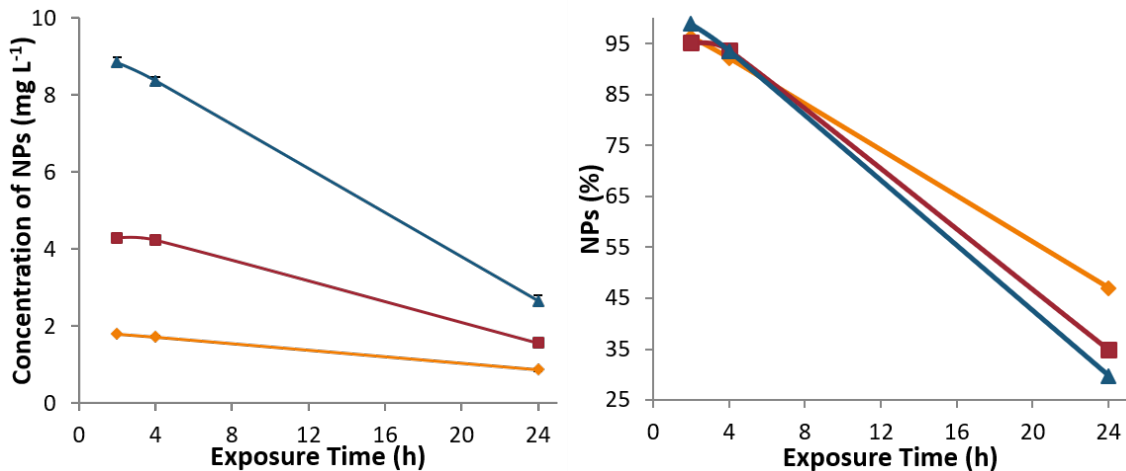


Figure 14 : (left) trend of NPs concentration (mg L<sup>-1</sup>) and (right) trend of NPs concentration (%) in the central part of water column for (◆)2, (■)5 and (▲)10 mg L<sup>-1</sup> samples as a function of time (2, 4 and 24 h).

### 2.2.3.3 CeO<sub>2</sub> in Elendt M7

The concentration profile at half water column height showed a trend similar to TiO<sub>2</sub>, but as expected more evident at the highest concentration, where there was an abrupt decrease of NPs detected with time of exposure, indicating the occurrence of a very fast sedimentation phenomena (Table 14 and Figure ).

Table 14 : Half water column height concentration expressed as Conc. center / Conc. total %, after 1, 24 and 48 hours of exposure in Elendt M7.

Concentration (mg L <sup>-1</sup> )	NPs percentage (%)		
	% 1h	% 24h	% 48h
0.02	100	100	95
0.2	89	79	59
2	100	50	16
5	93	29	4

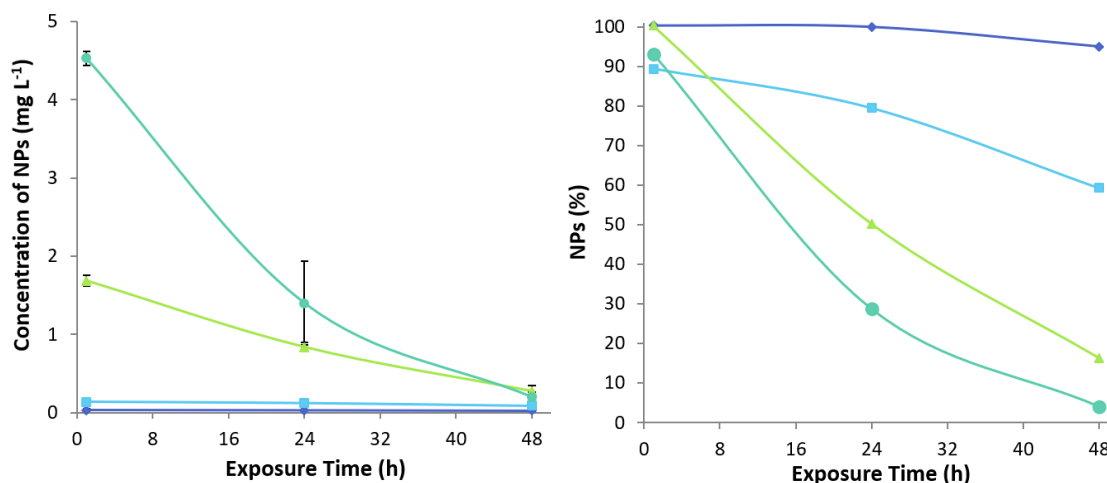


**Figure 15 :** (left) trend of NPs concentration (mg L<sup>-1</sup>) and (right) trend of NPs concentration (%) in the central part of water column for (♦) 0.02, (■) 0.2, (▲) 2 and (●) 5 mg L<sup>-1</sup> samples as a function of time (2, 24 and 48 h).

Thus, as compared to TiO<sub>2</sub>, CeO<sub>2</sub> presented a lower limit of stable concentration and therefore precipitated more quickly. Except for the 0.02 mg L<sup>-1</sup> sample, that preserved its stability and homogeneous NPs spreading (NPs percentage ≥ 95% in the 1h – 48h exposure range), all the other samples started to precipitate after the first hour. By 24h the samples presented a progressive decrease in NPs concentration, reaching in the case of the 5 mg L<sup>-1</sup> sample some unit percentage (4%) after 48h. Overall, CeO<sub>2</sub> NPs presented a high and progressive tendency to precipitate, driven by concentration and exposure time.

#### **2.2.3.4 Conclusions**

In this study, we investigated the sedimentation process of TiO<sub>2</sub> and CeO<sub>2</sub> in freshwater and seawater medium, mimicking the exposure conditions of ecotox *in-vivo* tests performed, respectively, with *Daphnia magna* and Zebrafish. A new set-up was optimised and validated with repeated measurements to estimate the concentration of ENMs at half water column height, in order to experimentally evaluate the sedimentation rate in a typical *in vivo* model and provide useful information for dosimetry adjustments.

#### **2.2.4 Particle size distribution via CLS measurements**

The CLS technique was used to determine the particle size distribution and the agglomeration state of ENMs in suspension, calculating hydrodynamic diameter. This parameter considers the environment of the particles and the solvation phenomenon. Many sources of uncertainties exist and can be related to sampling (weighing ENMs, volumetric operations such as pipetting,

and dilutions), calibration (purity of standards and of reagents), instrument performance, input parameters (density, viscosity, refractive index of ENMs, of standard, of media...), different operators, matrix effects and sample effects. Uncertainties could be calculated by using a bottom-up approach (identification of all uncertainty sources, combination of individual measurement) or a top-down approach (quantification of repeatability and intermediate precision only). Under our conditions, the top-down approach is more practical, however, it does not consider systematic errors. In order to evaluate reproducibility, an experiment was designed and was performed using this approach. A commercial solution from Benelux Scientific was used as a standard to avoid the errors related to the sampling. This solution contains PVC Nanoparticles with a certified size of 263 nm. This solution is homogenous and monodisperse; therefore, errors related to the matrix and samples effects may be avoided. Input parameters were found in the technical data sheet of the product. Measurements were performed 5 times for 5 consecutive days to minimise errors and to identify the uncertainties related to the instrument performance.

Particle size distribution are presented in different representations, in weight and/or in number of particles. Both representations appear in **Figure 16**. A bimodal distribution is observed in both cases (5 measurements per day during 5 days), but the signal is very narrow and is centered near 260 nm. Measurements are reproducible.

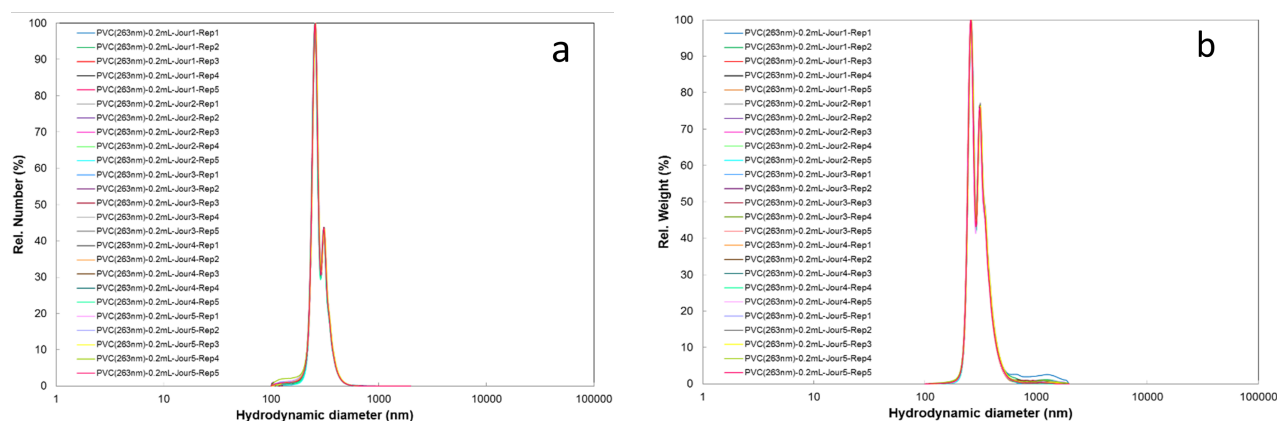


**Figure 16 : Particle size distribution (normalised) for PVC NPs (263 nm) provided by Benelux scientific a. in Number, b. in Weight related distributions.**

ANOVA treatment was used to calculate the uncertainty related to the instrument performance. It provides repeatability ( $S_{rep}$ ) and intermediate precision ( $S_{ip}$ ) values. A coverage factor ( $k$ ) of 2 was used in the calculations and the parameters  $n_{rep}$  and  $n_{days}$  are the number of replicates

and the number of days of measurements respectively. Mean square (MS) are calculated accordingly. Equations are described below.

$$S_{rep} = \sqrt{MS_{Within}}, S_{ip} = \sqrt{\frac{MS_{Between} - MS_{Within}}{n_{rep}}}$$

$$U_{ANOVA} = k \cdot \sqrt{\frac{S_{rep}^2}{n_{rep}} + \frac{S_{ip}^2}{n_{days}}}$$

$$U_{rel} = \frac{U}{Valeur} \times 100$$

Diameters of PVC NPs in both weight and number of particles are reported in **Table 15** and in **Table 16** respectively.

**Table 15 : Diameters of PVC NPs calculated by the CLS instrument from number related distributions.**

	Rep 1	Rep 2	Rep 3	Rep 4	Rep 5
<b>Day 1</b>	258.11	256.1	255.12	255.1	253.64
<b>Day 2</b>	257.59	257.1	256.66	255.97	255.25
<b>Day 3</b>	257.7	256.54	255.13	254.12	253.51
<b>Day 4</b>	257.4	256.47	255.31	255.31	253.99
<b>Day 5</b>	258.22	257.09	257.98	255.99	255.66

**Table 16 : Diameters of PVC NPs calculated by the CLS instrument from weight related distributions.**

	Rep 1	Rep 2	Rep 3	Rep 4	Rep 5
<b>Day 1</b>	261.08	258.96	258.23	257.85	256.61
<b>Day 2</b>	260.49	259.58	259.44	258.64	257.90
<b>Day 3</b>	260.54	259.3	257.8	256.73	256.05
<b>Day 4</b>	260.37	259.37	258.14	257.82	256.70
<b>Day 5</b>	261.34	260.12	260.66	258.57	258.19

ANOVA treatment was performed on the main intense signal only. Required data for ANOVA treatments are listed in **Table 17**. In number, the average value is  $256.03 \pm 2.82$  nm and in weight is  $258.78 \pm 2.97$  nm. The uncertainty related to the instrument is near 1.1 %, which is weak. From these results, we conclude that the CLS instrument is accurate and that the major

source of error (if errors is  $> 1.1\%$ ) comes mostly from the sampling stage.

**Table 17 : MS between and within group data are generated by ANOVA evaluation.  $S_{rep}$  and  $S_{ip}$  are calculated by using MS values in uncertainties equations.  $n_{rep}$  and  $n_{days}$  are assumed to be 1 for 1 measurement. The factor coverage k is assumed to be 2.**

	Number	Weight
<b>Average diameter (nm)</b>	256.03	258.78
<b><math>MS_{Between}</math></b>	2.291	2.248
<b><math>MS_{Within}</math></b>	1.907	2.188
<b><math>S_{rep}</math></b>	1.381	1.479
<b><math>S_{ip}</math></b>	0.277	0.110
<b><math>n_{rep}</math></b>	1	1
<b><math>n_{days}</math></b>	1	1
<b>K</b>	2	2
<b><math>U_{Mes}</math> (nm)</b>	2.82	2.97
<b><math>U_{rel}</math> (%)</b>	1.10	1.15

It would be suitable to use a top-down approach to calculate uncertainties for the particle size distribution of ENMs. This was tried; however, we often obtained an  $MS_{Within}$  value higher compared to  $MS_{Between}$ . This means that there are more errors within the same analysis group (replicates of the same day) than between different analyses groups (between different days). This result was not expected. Therefore, the ANOVA method was not a good approach to calculate uncertainties for our samples. One of the main reasons is that ENMs are not an “ideal” material. They are mostly in an agglomerated form; therefore, not homogenous in size and their dispersion in the medium is rarely reproducible, even if the protocol and the SOPs are followed accurately. The physico-chemical properties of the ENMs powder are quite sensitive, a bottle just opened compared to another stored for 1 week (even if it sealed it under Argon), may present different properties. In addition, any ENMs suspended in some media, tend after several minutes to agglomerate and/or sediment. Based on what is explained before, in this report and for CLS analyses, we prefer to express the uncertainties as standard deviations. The homogeneity within a vial (intra) and the homogeneity between vials (inter) were evaluated measuring a series of samples from different vials of a same ENM and prepared with the same procedure.

The NanoGENOTOX dispersion protocol and the SOP for calibration of Probe-sonicators for *in vitro* and *in vivo* testing were used for the suspension’s preparation. A stock solution of 2.56

mg/mL in water was prepared and was sonicated for 15.40 min using a Branson Sonifer S-450D (Branson Ultrasonics, 300Watt, 10% Ampl, 13 mm horn). A suspension of 0.1 mg/mL in Elendt M7 medium (preparation medium is based on OECD TG-211 (2012), OECD TG-202 (2004) and Elendt (1990), with minor modifications in methodology for practical reasons) was prepared from the stock solution. Analyses were performed with a gradient of sucrose in the proportion 2% and 8% and a speed of 22.000 rpm. A PVC NPs standard solution with a certified size of 263 nm was used for calibration and was injected before each analysis. A volume of 0.2 mL of sample was injected. Measurements were done in triplicates for 3 days. A total of 9 measurements were performed.

Average diameters in Number are presented in **Table 18**. The average diameter of TiO<sub>2</sub> remains near 12 nm whichever the environment and the suspension concentration. The full width at half maximum (FWHM) cannot be calculated for SiO<sub>2</sub> due to the broadness of the signal. ZnO uncoated and coated result in a similar diameter under the same conditions. The analysis of the particle size of MWCNT is more relevant in terms of weight; however, results in number were not reproducible.

**Table 18: Average diameter in Number evaluated by the CLS instrument of TiO<sub>2</sub> NM-105, SiO<sub>2</sub> NM-200, ZnO NM-110, ZnO NM-111 and MWCNT NM-402. Errors were calculated based on the standard deviation (s.d) on nine measurements (3 repetitions per day for 3 days).**

Material	Former NM code	Medium	Conc. (g/mL)	Average diameter in number (nm)	FWHM (nm)
TiO <sub>2</sub>	NM-105	H <sub>2</sub> O	2.56	12.1 ± 0.1	5.6 ± 0.0
TiO <sub>2</sub>	NM-105	H <sub>2</sub> O/BSA (0.05%)+EtOH	2.56	12.14 ± 0.04	5.59 ± 0.02
TiO <sub>2</sub>	NM-105	M7	0.1	12.2 ± 0.1	5.5 ± 0.1
SiO <sub>2</sub>	NM-200	M7	0.1	64 ± 0.4	/
ZnO naked	NM-110	M7	0.1	16 ± 1.3	11 ± 1.7
ZnO coated	NM-111	M7	0.1	16.5 ± 2.1	12.2 ± 1.9
MWCNT	NM-402 (990244)	M7	0.1	/	/
MWCNT	NM-402 (990700)	M7	0.1	/	/

Average diameters in Weight are presented in **Table 19**. In terms of weight, the diameter of TiO<sub>2</sub> primary particles remains unchanged. However, diameter of the agglomerates is strongly affected by the type of medium. In water, 5 populations of agglomerates can be observed.

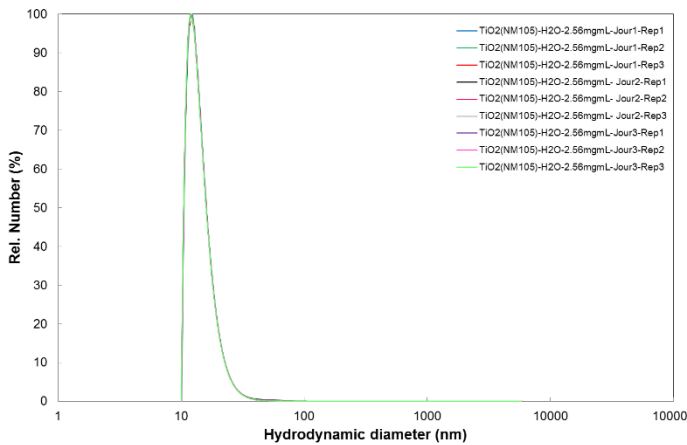
While, in the presence of BSA, only 1 population of agglomerate appears. In M7 medium, 2-3 populations of agglomerates are noticed. In general, water is not the best solvent to disperse TiO<sub>2</sub> ENMs; M7 medium is composed of mineral salts which are able to stabilise TiO<sub>2</sub> ENMs and BSA is known to have a dispersive effect on particles due to repulsive interactions. Therefore, it is not surprising to observe less agglomeration with BSA. A very broad signal is obtained for SiO<sub>2</sub> ENMs, with high-weight particles formed in M7 suspension. ZnO ENMs shows an additional population of agglomerates when it is coated. As expected, MWCNT show a signal near 500 nm.

**Table 19 : Average diameter in Weight evaluated by the CLS instrument of TiO<sub>2</sub> NM-105, SiO<sub>2</sub> NM-200, ZnO NM-110, ZnO NM-111 and MWCNT NM-402. Errors were calculated based on the standard deviation (s.d) on nine measurements (3 repetitions / day for 3 days). \* This peak does not appear in each replicate.**

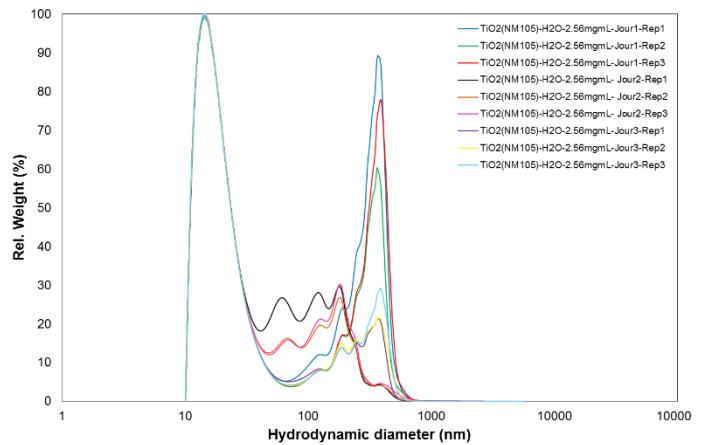
Materials	Former NM code	Medium	Conc. (g/mL)	Average diameter in weight (nm)	FWHM (nm)
TiO <sub>2</sub>	NM-105	H <sub>2</sub> O	2.56	Peak 1: 14.5 ± 0.1 Peak 2: 69.5 ± 4.8 Peak 3: 124.3 ± 2.9 Peak 4: 183.6 ± 4.1 Peak 5: 248.4 ± 1.8 Peak 6: 376.3 ± 1.2	12.6 ± 0.1
TiO <sub>2</sub>	NM-105	H <sub>2</sub> O/BSA (0.05%)+EtOH	2.56	Peak 1: 14.47 ± 0.02 Peak 2: 75.98 ± 21.21	12.72 ± 0.27
TiO <sub>2</sub>	NM-105	M7	0.1	Peak 1: 14.2 ± 0.4 Peak 2: 126.1 ± 0.6 Peak 3: 186.6 ± 2.3 Peak 4: 232.3 ± 7	12.5 ± 0.6
SiO <sub>2</sub>	NM-200	M7	0.1	Peak 1: / Peak 2: 1077.3 ± 101	/
ZnO Naked	NM-110	M7	0.1	Peak 1: 26.9 ± 1.3 Peak 2: 214.3 ± 2.1	182.7 ± 2.6
ZnO coated	NM-111	M7	0.1	Peak 1: 24.7 ± 3.2 (Peak 2: 156.4 ± 1.6)* Peak 3: 217.0 ± 25.3	187.8 ± 8.6
MWCNT	NM-402 (990244)	M7	0.1	Peak 1: 493.4 ± 16.1	363.6 ± 37.6
MWCNT	NM-402 (990700)	M7	0.1	Peak 1: 476.6 ± 35.5	361.3 ± 24.9

CLS spectra (distribution from number and weight related distributions of particles) of TiO<sub>2</sub> appear in **Figure** , SiO<sub>2</sub> and ZnO are presented in **Figure** and MWCNT are illustrated in Error! Reference source not found..

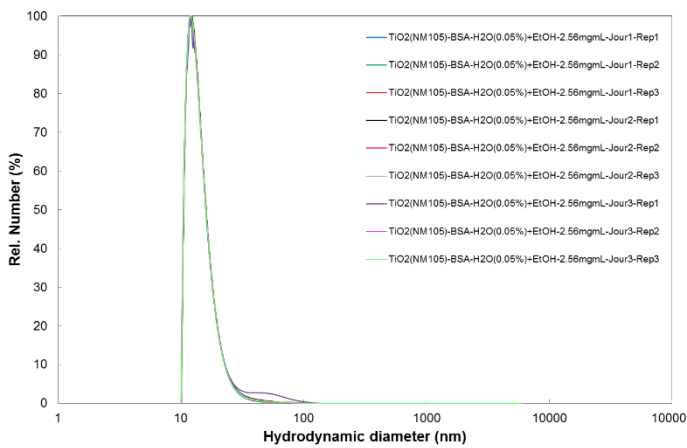
A1. TiO<sub>2</sub>\_NM-105\_H<sub>2</sub>O\_number



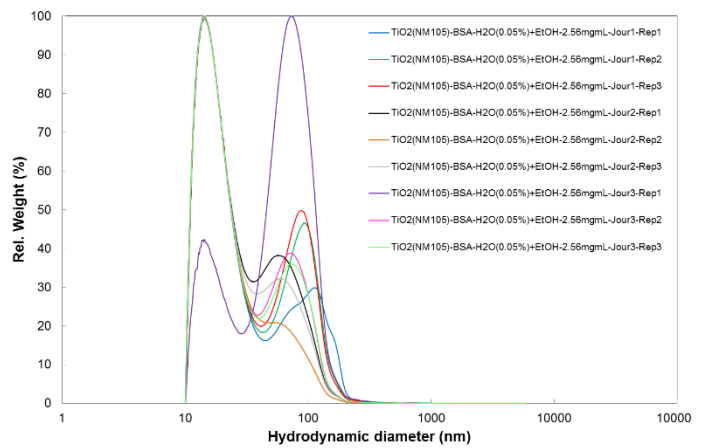
A2. TiO<sub>2</sub>\_NM-105\_H<sub>2</sub>O\_weight



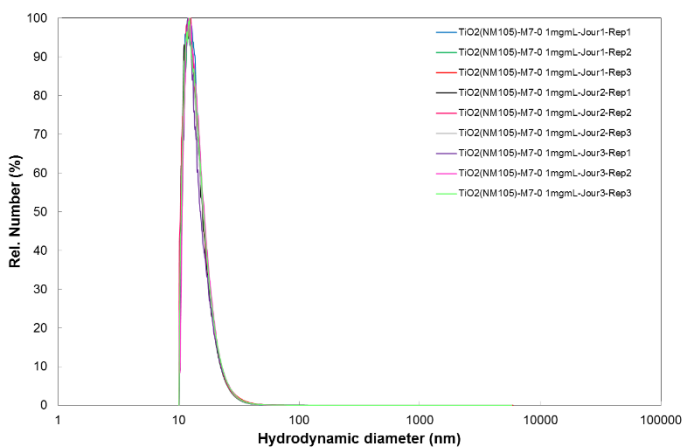
B1. TiO<sub>2</sub>\_NM-105\_H<sub>2</sub>O/BSA\_number



B2. TiO<sub>2</sub>\_NM-105\_H<sub>2</sub>O/BSA\_weight



C1. TiO<sub>2</sub>\_NM-105\_M7\_number



C2. TiO<sub>2</sub>\_NM-105\_M7\_weight

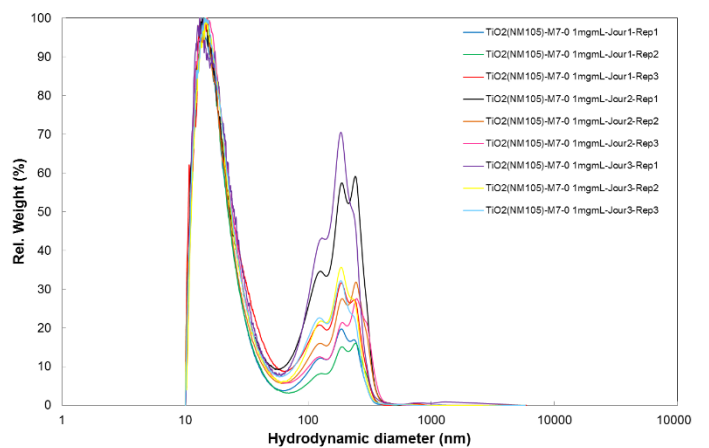
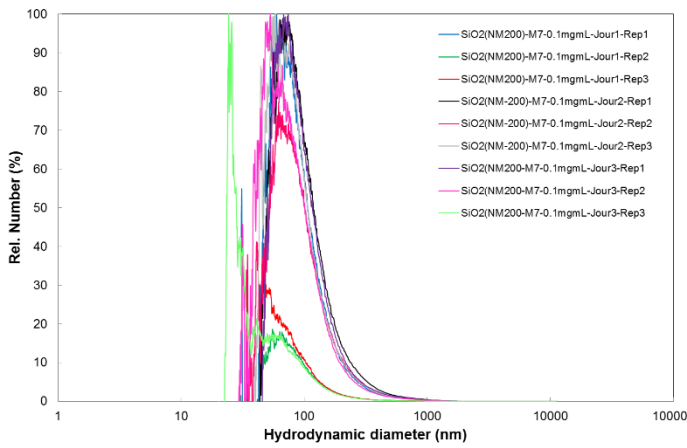
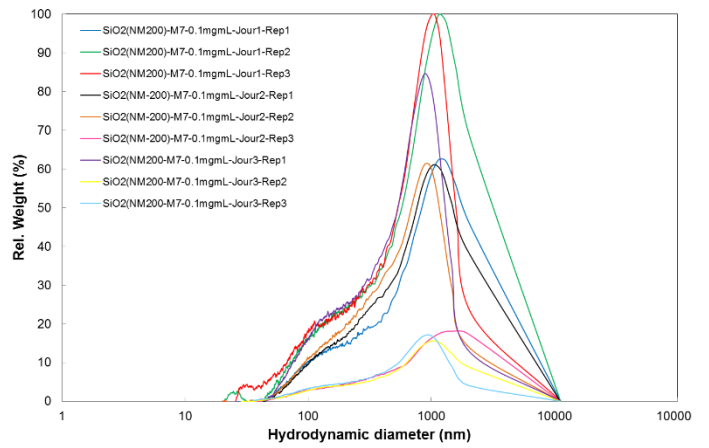


Figure 17 : CLS spectra (distribution in number and in weight) of TiO<sub>2</sub> NM-105 in water (A1, A2), in water/BSA (B1, B2) and in Elendt M7 (C1,C2).

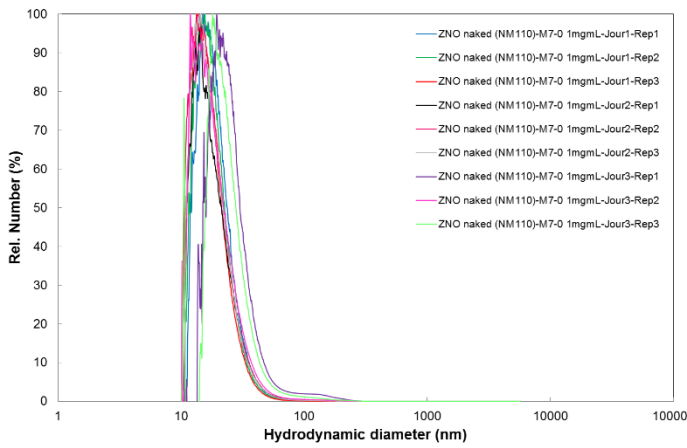
D1. SiO<sub>2</sub>\_NM-105\_M7\_number



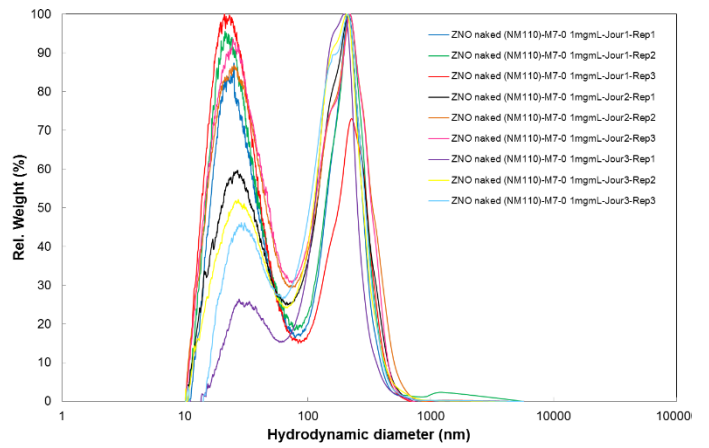
D2. SiO<sub>2</sub>\_NM-105\_M7\_weight



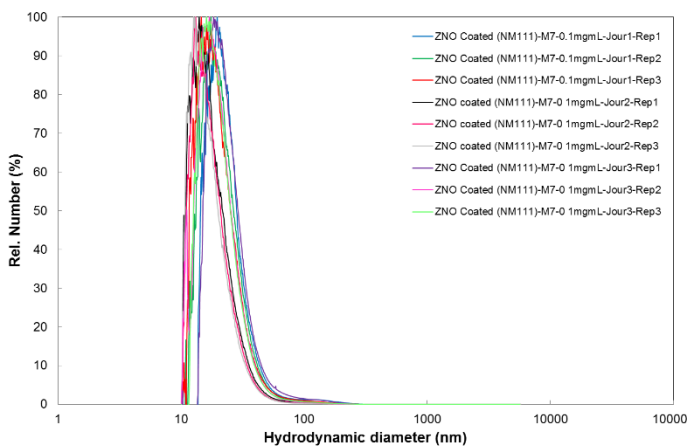
E1. ZnO\_NM-110\_M7\_number



E2. ZnO\_NM-110\_M7\_weight



F1. ZnO\_NM-111\_M7\_number



F2. ZnO\_NM-111\_M7\_weight

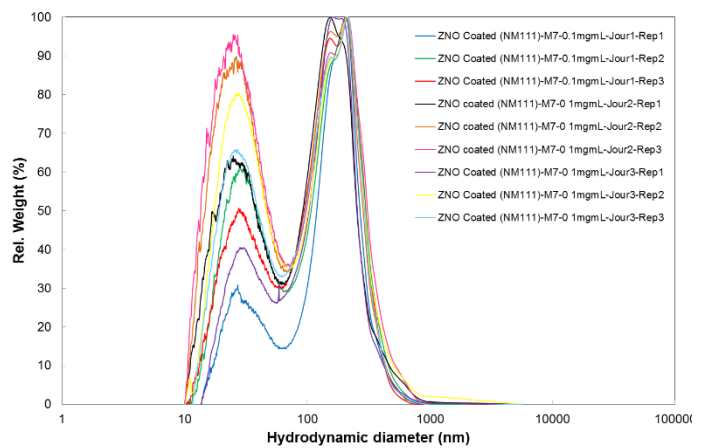
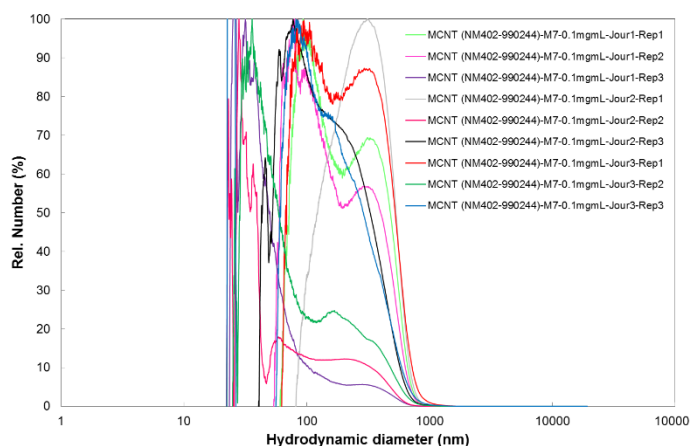
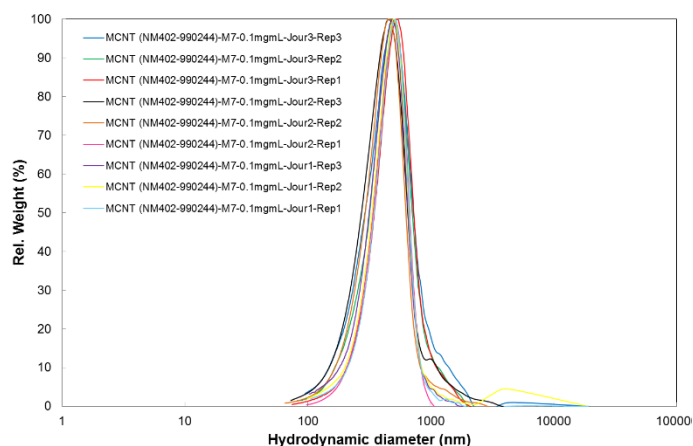


**Figure 18: CLS spectra (distribution in number and in weight) in M7 of SiO<sub>2</sub> NM-200 (D1, D2), of ZnO NM-110 (E1, E2) and of ZnO NM-111 (F1,F2).**

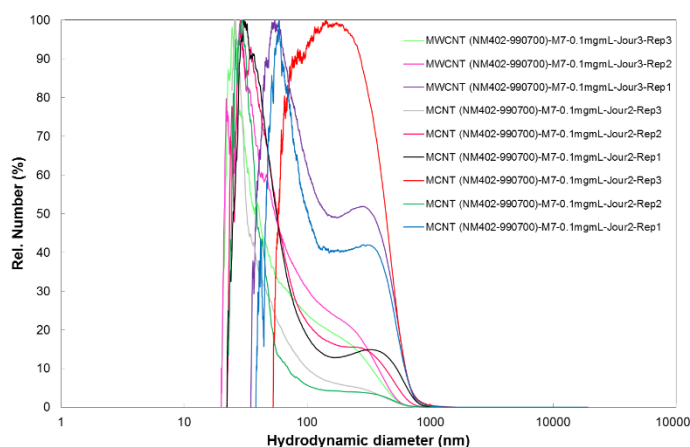
G1. MWCNT\_NM-402(990244)\_M7\_number



G2. MWCNT\_NM-402(990244)\_M7\_weight



H1. MWCNT\_NM-402(990700)\_M7\_number



H2. MWCNT\_NM-402(990700)\_M7\_weight

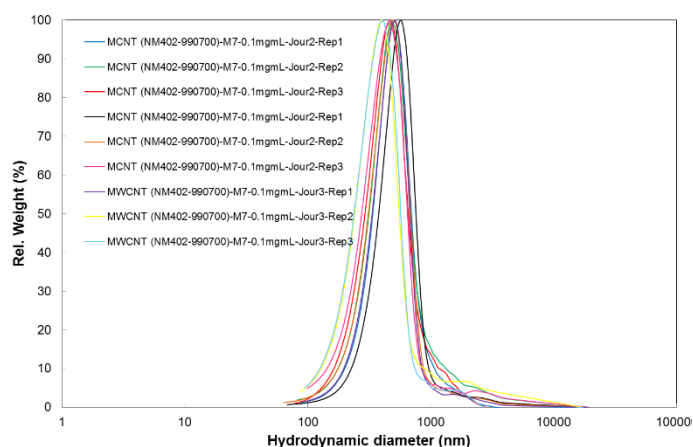


**Figure 19: CLS spectra (distribution in number and in weight) in M7 of MWCNT NM-402-990244 (G1, G2) and of NM-402-990700 (H1, H2).**

Weight related distributions highlights the presence of the agglomerates (big in size and smaller in number) of the sample. In the number related distribution, those same agglomerates will be overcome by the large number of nanoparticles (lower in weight). It is worth mentioning that conversion between weight and number related distributions are performed by mathematical transformations. Therefore, these numerical representations need to be considered cautiously and only for comparison purposes among similar samples or in the same series of results. Another aspect, that cannot still be mastered is that the whole distribution of particles relates to a nominal density. This is an approximation, given that the density of the agglomerates will be different from those of the primary particles.

In the literature, particle size distributions of these ENMs are mostly evaluated with the DLS technique. Thus, conditions such as: type of medium, sample volume and concentration are

not always the same as with our experiments (CLS technique). For TiO<sub>2</sub> ENMs, JRC reports a Z-average diameter in ultra-pure water dispersion (ultrasonic bath) of 554.9 nm and of 155 nm, using an ultrasonic tweeter. For SiO<sub>2</sub> ENMs, the Z-average diameter in milliQ water dispersion is 136 nm (peak 1) and 376 nm (peak 2). In culture media dispersion, the Z-average is 144.4 (peak 1) and 2611 nm (peak 2). For ZnO NM-110, a Z-average diameter of 275±4 in milliQ water is reported. For ZnO NM-111, the Z-average diameter is 253±1. DLS measurements show a unimodal distribution for ZnO uncoated but a bimodal distribution for the coated one. The hydrodynamic diameter measured by CLS for ZnO NM-110 in daphnia medium (= Elendt M7) is 296 ± 16 nm. Concerning MWCNT, no comparison with JRC report can be made because the diameter and length of the tubes were only evaluated by TEM instrument. In conclusion, our CLS data correspond with those results found in the literature.

### **2.2.5 Turbiscan measurements and determination of sedimentation rate**

The Turbiscan LAB™ instrument can scan the entire height of a sample tube to record transmission (T) and backscattering (R)<sup>31</sup>. This instrument provides identification and tracking of the destabilisation phenomena of complex systems. Sedimentation phenomenon can be observed when the density of the dispersed phase is greater than the density of the continuous phase.

The calculation of the sedimentation rate is based on the Turbiscan Stability Index (TSI) value. This parameter is a useful tool to compare multiple samples. The calculation of the TSI is based on the comparison of each scan with the previous one, according to the formula below. Each scan at a given height is subtracted from the previous scan at the same height; the whole is integrated and divided by the total height of the sample. In this way, all the signal variations are considered and a number that reflects the “sample destabilisation” is obtained. The higher the TSI value, the less stable is the sample.

$$TSI = \frac{\sum_h |Scan_i(h) - Scan_{i-1}(h)|}{H}$$

The NanoGENOTOX dispersion protocol and the SOP for calibration of Probe-sonicators for *in vitro* and *in vivo* testing were used for the suspension's preparation. A stock solution of 2.56 mg/mL in water was prepared and was sonicated for 15.40 min using a Branson Sonifer S-450D (Branson Ultrasonics, 300Watt, 10%Ampl, 13 mm horn). A suspension of 0.1 mg/mL in Elendt M7 medium (preparation medium is based on OECD TG-211 (2012), OECD TG-202 (2004) and Elendt (1990), with minor modifications in methodology for practical reasons) was prepared from the stock solution. A volume of 20 mL was analysed and was recorded for 24h.

Turbiscan analysis is highly dependent on the quality of the dispersion protocol, the ENMs turbidity and their physico-chemical properties. To illustrate this, two TiO<sub>2</sub> NM-105 dispersions in water prepared with the same protocol at a concentration of 2.56 mg/mL may behave in a different way. In Error! Reference source not found. more sedimentation is observed in the right vial compared to the left one.



**Figure 20: Suspensions of TiO<sub>2</sub> NM-105 particles suspended in water at a concentration of 2.56 mg/mL.**

The time-dependent evolution of TSI values is described in Error! Reference source not found.<sup>1</sup> After 5h of sedimentation, a TSI near 5 is obtained for the SiO<sub>2</sub> suspension, about 30 for MWCNT, near 40 for both ZnO suspensions and near 60 for TiO<sub>2</sub>. The stability of these ENMs in suspension increases as TiO<sub>2</sub> < MWCNT < ZNO < SiO<sub>2</sub>. Thus, SiO<sub>2</sub> ENMs are more stable and has a sedimentation rate slower compared to the others. In all cases, the sedimentation process stops after 24h. This means that a 24h experiment is enough to study the sedimentation phenomenon. The sedimentation reaches stability after 8h for SiO<sub>2</sub>, after 17h for MWCNT, after 11h for ZnO and after 19h for TiO<sub>2</sub>. In the case of SiO<sub>2</sub> NM-200, this result was not expected. This dispersion is composed mostly of agglomerates-aggregates of a large size and agglomeration is known to govern mass transport motion as sedimentation<sup>31</sup>. The conclusion of this experiment is that SiO<sub>2</sub> ENMs are better dispersed in the M7 medium, in contrast to the TiO<sub>2</sub> ENMs.

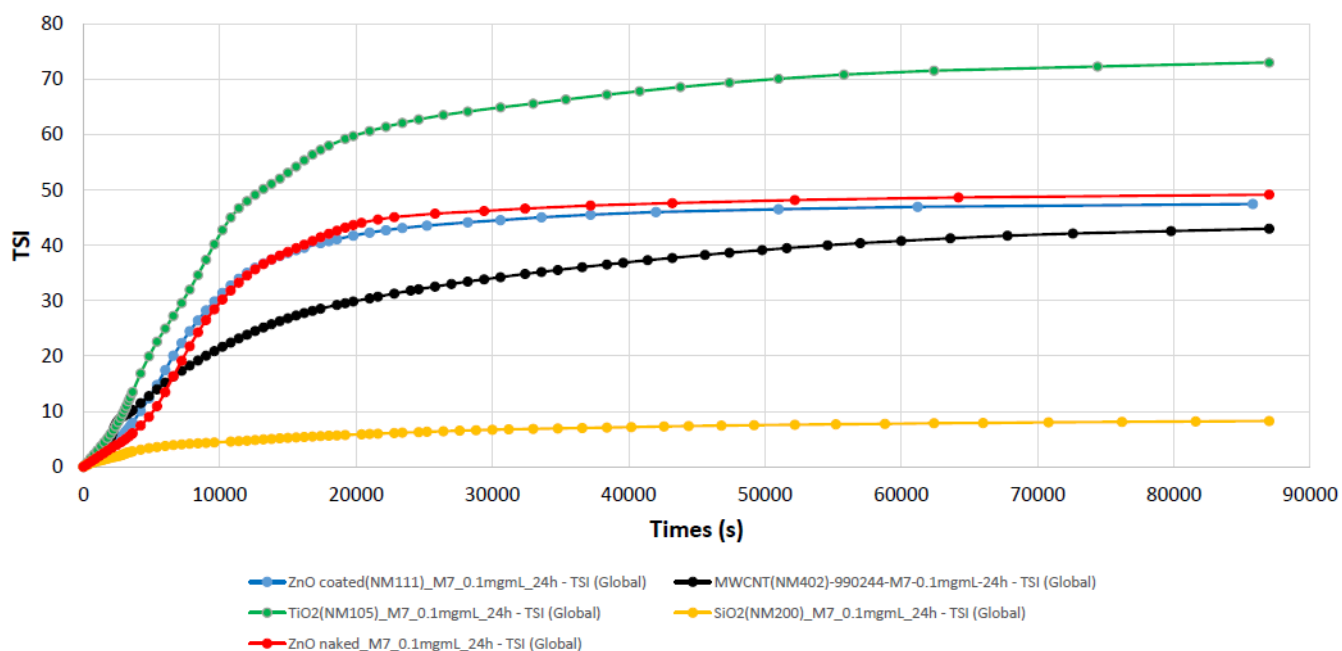


**Figure 21: Evolution of the TSI value as function of time of TiO<sub>2</sub> NM-105, SiO<sub>2</sub> NM-200; ZnO NM-110, ZnO NM-111 and MWCNT NM-402 ENMs in suspension in Elendt M7 medium at the concentration of 0.1 mg/mL.**

### 2.3 Dosimetry analysis of ecotox suspensions

In the collaboration with Dr Nathaniel Clark at the University of Plymouth, UNEXE carried out fate and dosimetry analyses for three different ENM suspensions, AgNP (NM300K, JRC), PVP-coated AgNP (CENR) and ZnONP (NM110, JRC), in zebrafish culture media (Egg Water). The three ENMs were chosen on the basis that we found AgNP and ZnONP acted as potent inducers of oxidative stress in our pilot acute exposure assay to selected ENMs using the embryos of the oxidative stress (EpRE) biosensor transgenic zebrafish (Mourabit *et al.*, 2019). The analysis we present here on the behaviour of these metal nanomaterials complements the mode of action studies for these ENMs in zebrafish embryo-larvae conducted under WP5 (deliverable WP5.2). To characterise the dosimetry of these selected ENMs, we analysed the following: 1) total metal concentration in exposure media, 2) total metal concentration in experimental animals (4 day-old zebrafish larvae), 3) particle size in ENM suspension and 4) dissolution kinetics of ENM in the embryo-larval culture media.

UNEXE prepared all samples for the measurement of total metal in the exposure media (two different doses in replicate (N=4), sampled at 0, 24, 48 and 72h after the initiation of the exposure) and in exposed zebrafish embryo-larvae (prepared at the end of the acute exposure). In addition, AgNO<sub>3</sub> and ZnSO<sub>4</sub>·7H<sub>2</sub>O were used for the acute exposure as ion control solutions. The samples for total metal measurements in exposure media and in

exposed zebrafish larvae for these controls were prepared in a similar manner as described for ENM samples. Collected exposure media were digested with Nitric Acid (Primer Plus, Fisher Scientific, final 17.6% in the water sample) immediately after sampling at each time point and stored at 4°C until analysis (this was done for all samples for any given exposure study at the same time after the final sample collection). Collected water samples were transported to Plymouth University where they were analysed using SM-ICP-MS. Samples for total metal measurements in 4 dpf (days post fertilisation) zebrafish larvae were freeze-dried and stored at -20°C until analysed subsequently using SM-ICP-MS analyses.

Particle sizes for PVP-coated and uncoated AgNP and ZnONP suspensions were measured using Nanoparticle Tracking Analysis (NTA) at Plymouth University. For this stock ENM suspensions (which were prepared one day prior to each exposure assay) were diluted in either ultrapure water or Egg Water to an appropriate mass concentration to measure a sufficient number of particles (i.e. for AgNP [NM300K], 2.56mg/ml for stock concentration and 1mg/L for diluted concentration for NTA analysis). The particle size measurements by NTA were conducted immediately following dilution.

Dissolution kinetics for the ENM suspensions were measured in Egg Water by filter dialysis method. The diluted ENM solution was placed in a filter bag and the bag was incubated in a small beaker filled with the same Egg water. These kinetic studies were conducted in triplicate and samples were collected for analysis at 0, 0.25, 0.5, 1,2,4,24, 48 and 72 hours to measure the dissolved metal concentration in the Egg Water.

### ***2.3.1 Total metal concentrations in the Egg Water***

Measured concentrations of silver and zinc in the Egg Water are shown in **Table 20**. For the silver ENMs measured levels were less than nominals throughout. For PVP-AgNPs the measured levels were consistent across the incubation period (over 72h). This was also the case for the AgNP NM300k for the higher exposure dose, but at the lower dosing the level dropped considerably over the 72h incubation period. Levels of total Ag in the AgNO<sub>3</sub> incubations were considerably lower than nominals for both exposure dosings but relatively consistent over the 72h incubation period.

For the zinc ENMs measured levels were less than nominals throughout in the higher dosing and higher for the lower level dosing. Again however, the measured levels were consistent for both dosing levels across the incubation period (over 72h). Levels of total Zn in the

ZnSO<sub>4</sub>·7H<sub>2</sub>O incubation were lower than nominals for both exposure dosings but relatively consistent over the 72h incubation period.

**Table 20: Total metal measurement by SM-ICP-MS for AgNP (NM300K, JRC), PVP-coated AgNP (CENR) and ZnONP (NM110, JRC) suspensions and ion control solution (AgNO<sub>3</sub> and ZnSO<sub>4</sub>·7H<sub>2</sub>O in zebrafish exposure media (Egg Water) over a 72h incubation period.**

AgNP (NM300K, JRC)	measured conc of total Ag (µg/L)		
Time	water control	nominal AgNP 33µg/L	nominal AgNP 330µg/L
0h	<LOD*	20.28±0.13	110.20±9.77
24h	<LOD*	13.27±3.11	129.81±10.36
48h	<LOD*	8.58±1.77	142.50±5.40
72h	<LOD*	6.73±1.66	115.328±8.30

\*Limit Of Detection

PVP-AgNP(CENR)	measured conc. of total Ag (µg/L)		
Time	water control	nominal AgNP 33µg/L	nominal AgNP 330µg/L
0h	<LOD*	21.93±2.40	176.99±6.82
24h	<LOD*	26.37±4.52	199.62±15.05
48h	<LOD*	24.60±1.27	190.54±24.63
72h	<LOD*	25.48±4.08	279.59±9.99

\*Limit Of Detection

AgNO <sub>3</sub>	measured conc. of total Ag (µg/L)		
Time	water control	nominal AgNO <sub>3</sub> 3.3µg/L	nominal AgNO <sub>3</sub> 33µg/L
0h	<LOD	0.51±0.02	8.83±0.61
24h	<LOD	0.52±0.05	8.47±0.75
48h	<LOD	0.51±0.39	5.68±5.51
72h	<LOD	0.74±0.83	5.16±4.14

\*Limit Of Detection

ZnONP(NM110m JRC)	measured conc. of total Zn (µg/L)		
Time	water control	nominal ZnONP 33µg/L	nominal ZnONP 1mg/L
0h	18.69±6.54	48.24±17.90	706.00±16.18
24h	26.52±7.67	49.75±5.50	738.64±17.10
48h	25.53±5.49	52.95±11.55	766.93±40.66
72h	26.31±4.66	68.61±31.76	762.00±18.18

ZnSO <sub>4</sub> ·7H <sub>2</sub> O	measured conc. of total Zn (µg/L)		
time	water control	nominal ZnSO <sub>4</sub> ·7H <sub>2</sub> O 100µg/L	nominal ZnSO <sub>4</sub> ·7H <sub>2</sub> O 10mg/L
0h	18.69±6.54	45.83±0.02	2534.14±19.20
24h	26.52±7.67	60.15±0.05	2492.78±63.09

48h	25.53±5.49	51.92±0.39	2531.75±106.87
72h	26.31±4.66	42.24±0.83	2661.21±39.11

### 2.3.2 Particle sizes in Egg Water

**Figure** shows an example of the NTA analysis for AgNP (NM300K) in Egg Water. While NTA average particle size measurements for the tested ENM in suspension are shown in **Table 21**.

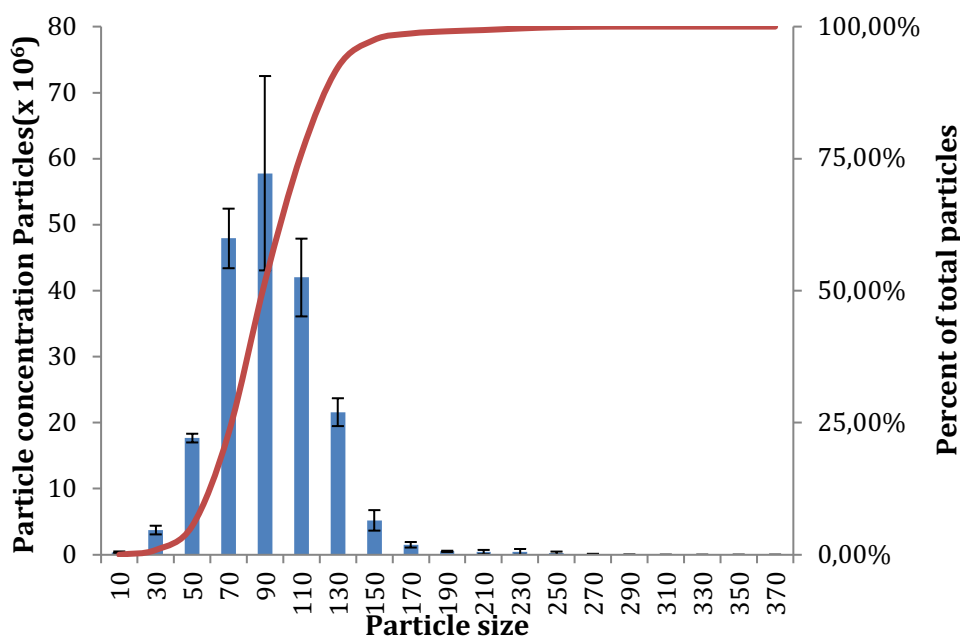


**Figure 22 : Example of NTA analysis for particle diameter measurement – AgNP (NM300K) in Egg Water**

**Table 21: NTA particle size measurement**

sample	Water	average particle size (nm)
PVP-coated AgNP (CENR)	ultrapure water	82.3±4.67
	Egg Water	104.7±8.41
AgNP (NM300K, JRC)	ultrapure water	88±1.73
	Egg Water	91.3±0.33
ZnONP (NM110, JRC)	ultrapure water	142.7±8.69
	Egg Water	147±10.6

### 2.3.3 Dissolution Analysis in Egg Water

The dissolution assays revealed that there was no detectable total Ag release from PVP-AgNP

(detection limit of the SM-ICP-MS was  $0.05\mu\text{g/L}$ ) in Egg Water for all time points, suggesting that PVP-coated AgNP did not dissolve and remained in particulate form in the zebrafish media over 72 hours.

Non-coated AgNP (NM300K) showed no detectable dissolution in Egg Water before 24h and very little dissolution between 24h and 72h (i.e.  $0.06\pm 0.03\%$  at 24h vs  $0.12\pm 0.03\%$  at 72h). These data indicate that AgNPs are generally stable and largely remain in particulate form in Egg Water throughout the period of the acute exposure assay.

In contrast, ZnONP (NM110, JRC) showed marked dissolution in Egg Water over time, leading to  $78.2\pm 3.7\%$  dissolution at 72h (**Figure** ).

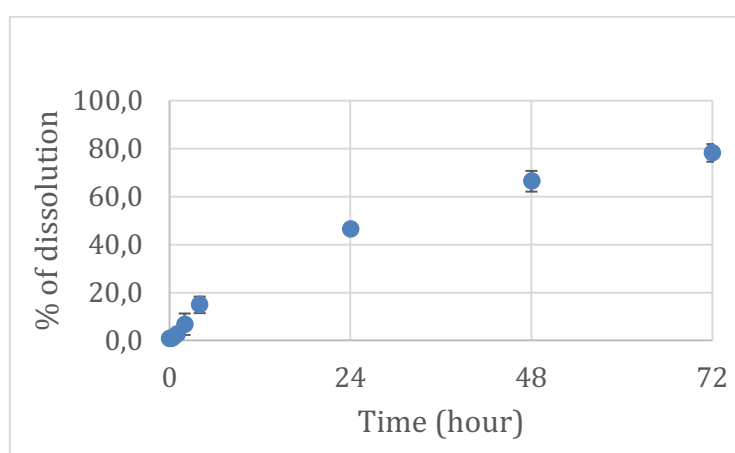


**Figure 23: Dissolution of ZnONP (NM110) in Egg Water.**

These data show considerable differences in the fate of the silver and zinc ENMs in the zebrafish embryo-larval culture medium with major implications for biological effect analyses.

#### **2.3.4 Total metal content in exposed zebrafish embryo-larvae**

No silver was detected in the bodies of control embryo-larvae. In contrast around 7ng Zn/embryo larvae was measured in controls, consistent with that expected given the role of endogenous Zn in many physiological processes. **Figure** shows that Ag and Zn were clearly uptaken into the embryo larvae in dose dependent manners. Interestingly, at the higher dosing level, PVP-coated silver appeared to be more bioavailable to zebrafish embryo larvae compared with non-coated AgNP. We have not established in what form the silver is taken up into the body tissues or resides in body tissues for these ENMs.

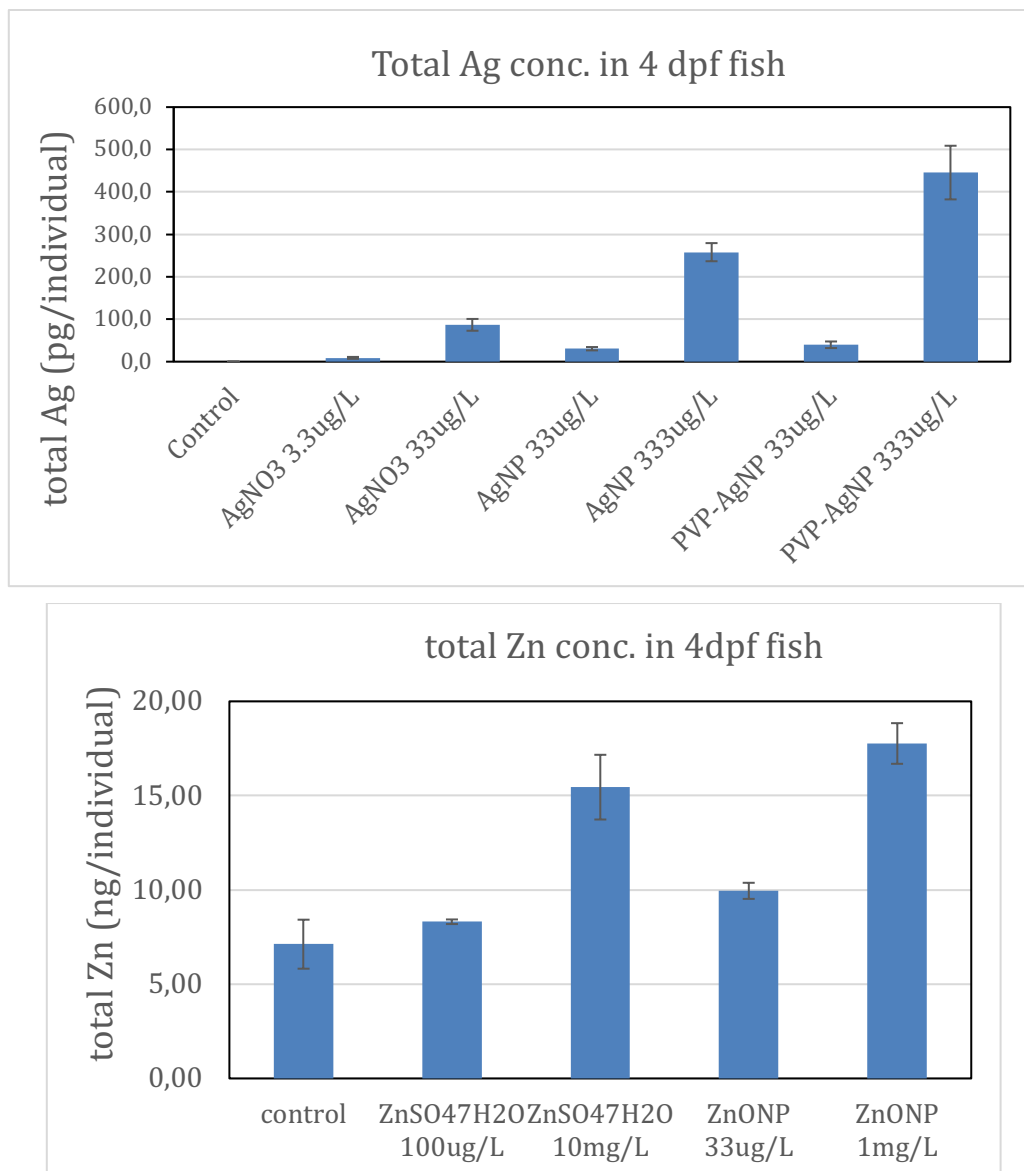


**Figure 24: Total metal measurement by SM-ICP-MS in 4 dpf zebrafish larvae exposed with AgNP (NM300K, JRC), PVP-coated AgNP (CENR), ZnONP (NM110, JRC) or ion control solution (AgNO<sub>3</sub> and ZnSO<sub>4</sub>·7H<sub>2</sub>O) in Egg Water for 4 days.**

### 2.3.5 Fate assessment of nZnO for long-term *Daphnia magna* tests

Evaluation of ENMs exposure in complex media, under realistic conditions, will provide understanding on the nano-bio-interphase. These parameters may influence parameters such as: ENMs physico-chemical properties, mobility, stability, dosimetry, fate and bioavailability over time. ZnO NM-111 ENMs was selected to study sedimentation process, agglomerate state and particle size distribution in water suspension and in *Daphnia* medium (Elendt M7) with the CLS instrument. Analyses were performed with a gradient of sucrose, composed of a mixture of 2% and 8% dispersions, and a speed of 22.000 rpm. A certified PVC standard solution with a size of 263 nm was used for calibration (0.1 mL) and was injected before each

analysis. A sample volume of 0.2 mL was injected.

The NanoGENOTOX dispersion protocol and the SOP for calibration of Probe-sonicators for *in vitro* and *in vivo* testing were used for the suspension's preparation. A stock solution of 2.56 mg/mL in water was prepared and was sonicated for 15.40 min using a Branson Sonifer S-450D (Branson Ultrasonics, 300Watt, 10%Ampl, 13 mm horn). A suspension of 0.1 mg/mL in Elendt M7 medium (preparation medium is based on OECD TG-211 (2012), OECD TG-202 (2004) and Elendt (1990), with minor modifications in methodology for practical reasons) was prepared from the stock solution.

Sampling was done at 4 different times: 0h, 3h, 6h and 24h and at 3 different heights: Top (1.6 cm from the top reference), Middle (2.6 cm from the top reference) and Bottom (3.8 cm from the top reference). The vial dimensions are 2 cm wide by 4cm length. Experiments were performed in 2 different media: water and daphnia medium (Elendt M7). The experimental design is shown in **Figure** .

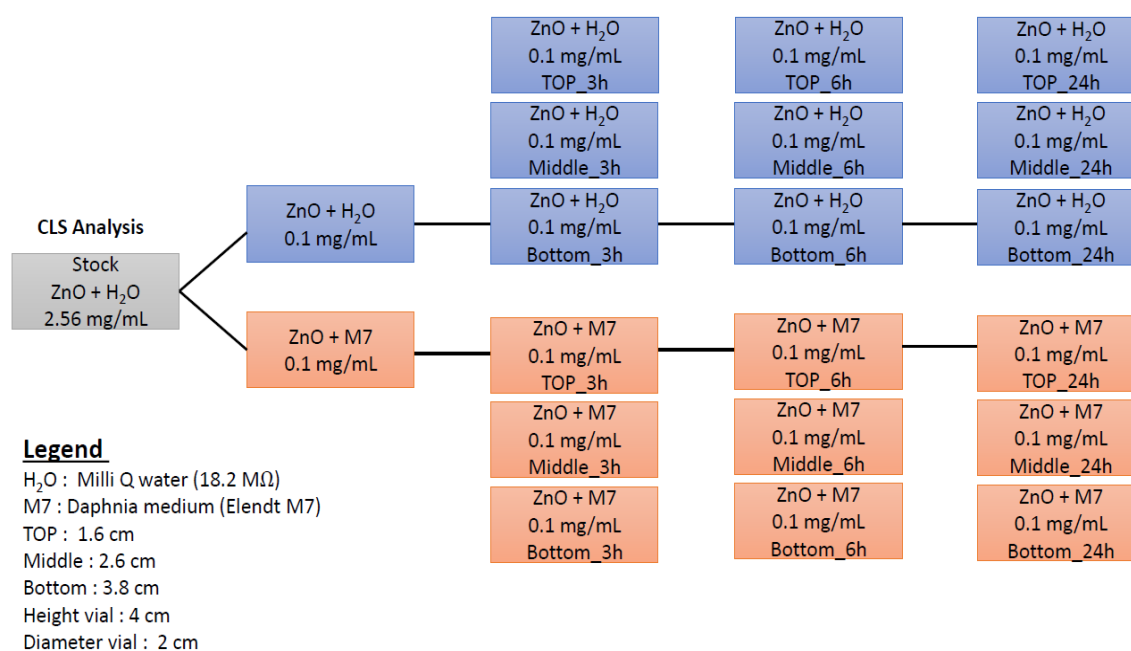


**Figure 25: Experimental scheme of the analysis of the particle size distribution by the CLS technique of ZnO NM-111 in H<sub>2</sub>O and in M7 at different times (0, 3, 6 and 24h) and at different heights of the vial (Top, Middle and Bottom).**

Particle size distributions in weight and in number related distributions of ZnO ENMs in stock H<sub>2</sub>O solution are presented in

**Table 22** and in **Figure** . Two main populations of particles are observed in the weight related distribution. One population at about 21 nm which corresponds to the primary particle (PP) and

a second one at about 216 nm which correspond to the agglomerates (Agglo). In the number related distribution, a unimodal distribution is observed and is centered at about 13 nm.

**Table 22 : Diameter of primary particles (PP) and agglomerates (Agglo) of ZnO NM-111 suspended in H<sub>2</sub>O (2.56 mg/mL).**

Stock H <sub>2</sub> O (2.56 mg/mL)		
	Diameter PP (nm)	Diameter Agglo (nm)
<b>Weight</b>	21.40	216.1
<b>Number</b>	12.90	/

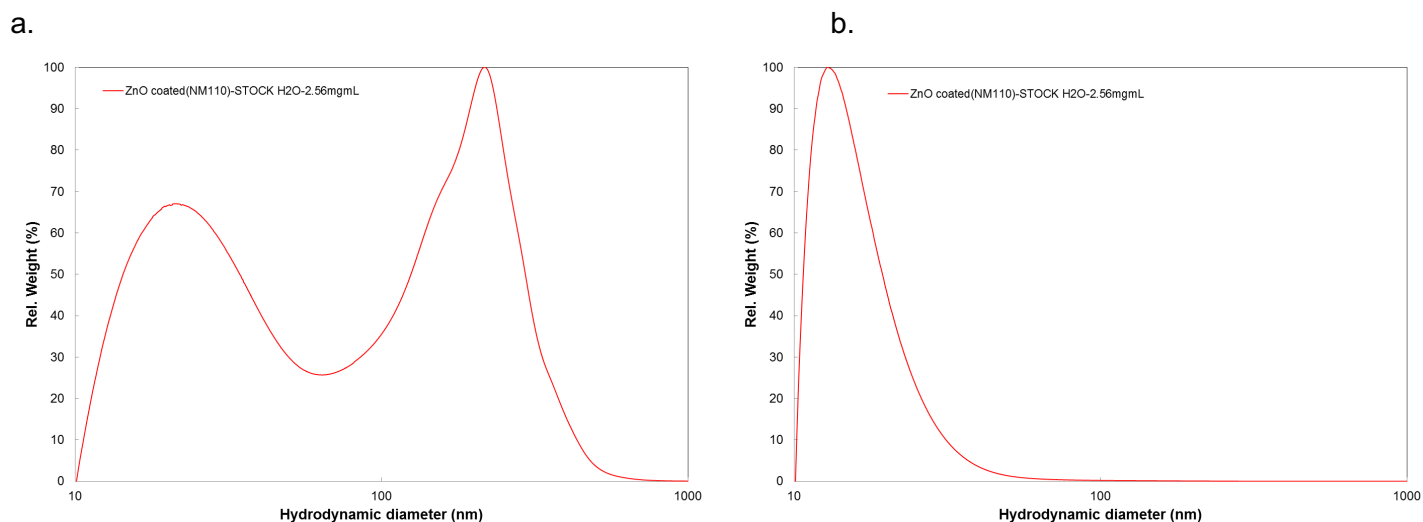


**Figure 26 : Particle size distribution, a. Weight related distribution, b. Number related distribution of ZnO NM-111 suspended in H<sub>2</sub>O (2.56 mg/mL).**

Diameter values for ZnO ENMs in water suspension (0.1mg/mL) over time and height, are reported in weight related distribution only and are shown in

**Table 23.** Results, either for height or time, are illustrated in **Figure** and in **Figure** respectively.

**Table 23: Diameter of primary particles (PP) and agglomerates (Agglo) of ZnO NM-111 suspended in H<sub>2</sub>O (0.1 mg/mL).**

Medium: H <sub>2</sub> O (0.1 mg/mL)		
TOP_Weight	Diameter PP (nm)	Diameter Agglo (nm)
0h	24	151; 200
3h	34	148
6h	/*	138
24h	/*	/*
Middle_Weight		
0h	24	151; 200
3h	28	144
6h	/*	139
24h	/*	88
Bottom_Weight		
0h	24	151; 200
3h	30	134
6h	23	131
24h	/*	112

\* Non detected values

The PP than Agglo, present at the beginning of the experiment (time 0h), decrease over time, especially at the top of the vial. At the beginning, the sedimentation process seems to be faster in the upper layer. After 24h, no more PP and Agglo can be detected. All the agglomerates have disappeared from the top and are detected in the bottom of the vial, which is the evidence of sedimentation. While PP seem to be transformed into agglomerates during the sedimentation process, no PP are detected later in any layer. These results indicated that PP seem to be more affected by sedimentation. This result is surprising as agglomerates are known to sediment faster, but if medium is entrapped inside, the effective density of these agglomerates will decrease and consequently, they will sediment slowly.

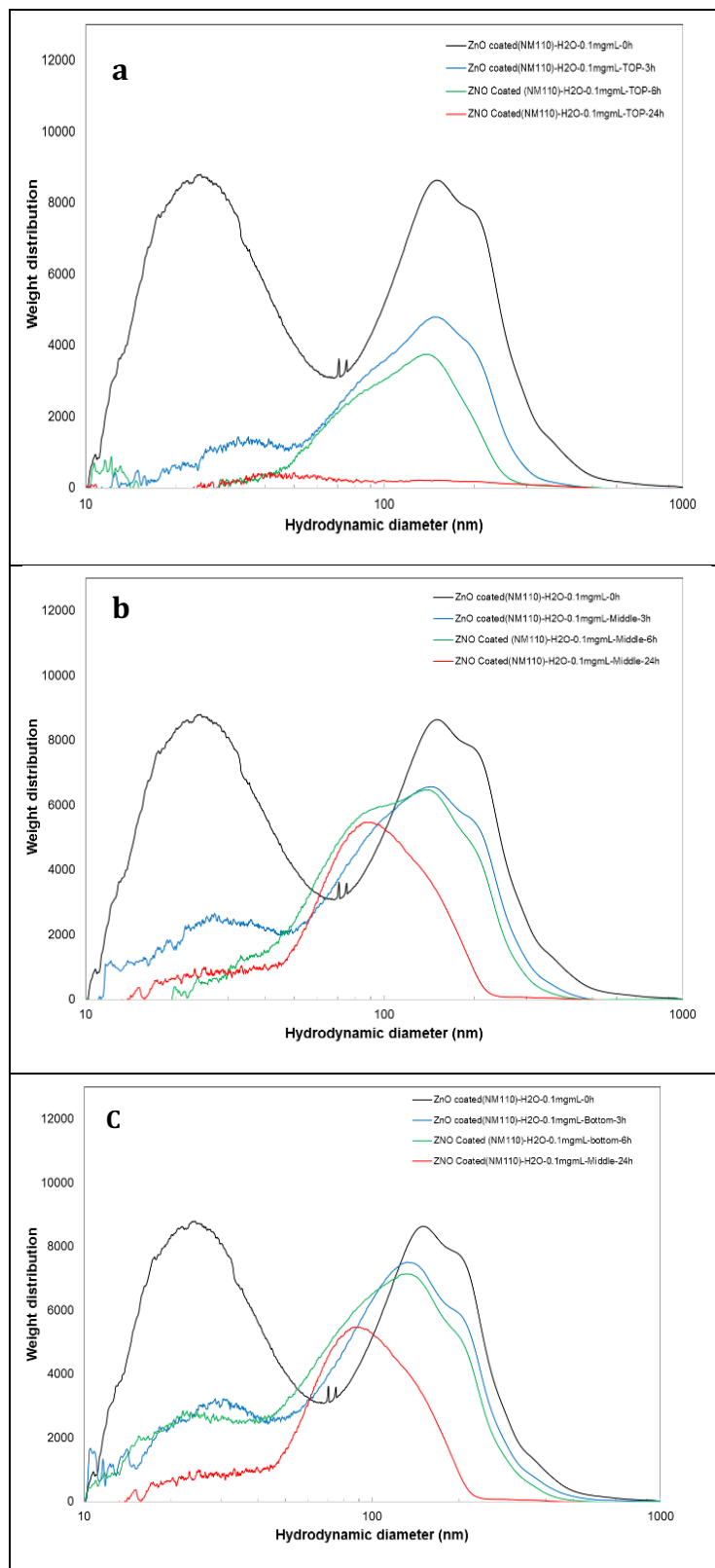


**Figure 27 : Particle size distribution of ZnO NM-111 in H<sub>2</sub>O (0.1 mg/mL) at different times (0, 3, 6 and 24h), with a fixed height a. Top, b. Middle, c. Bottom.**

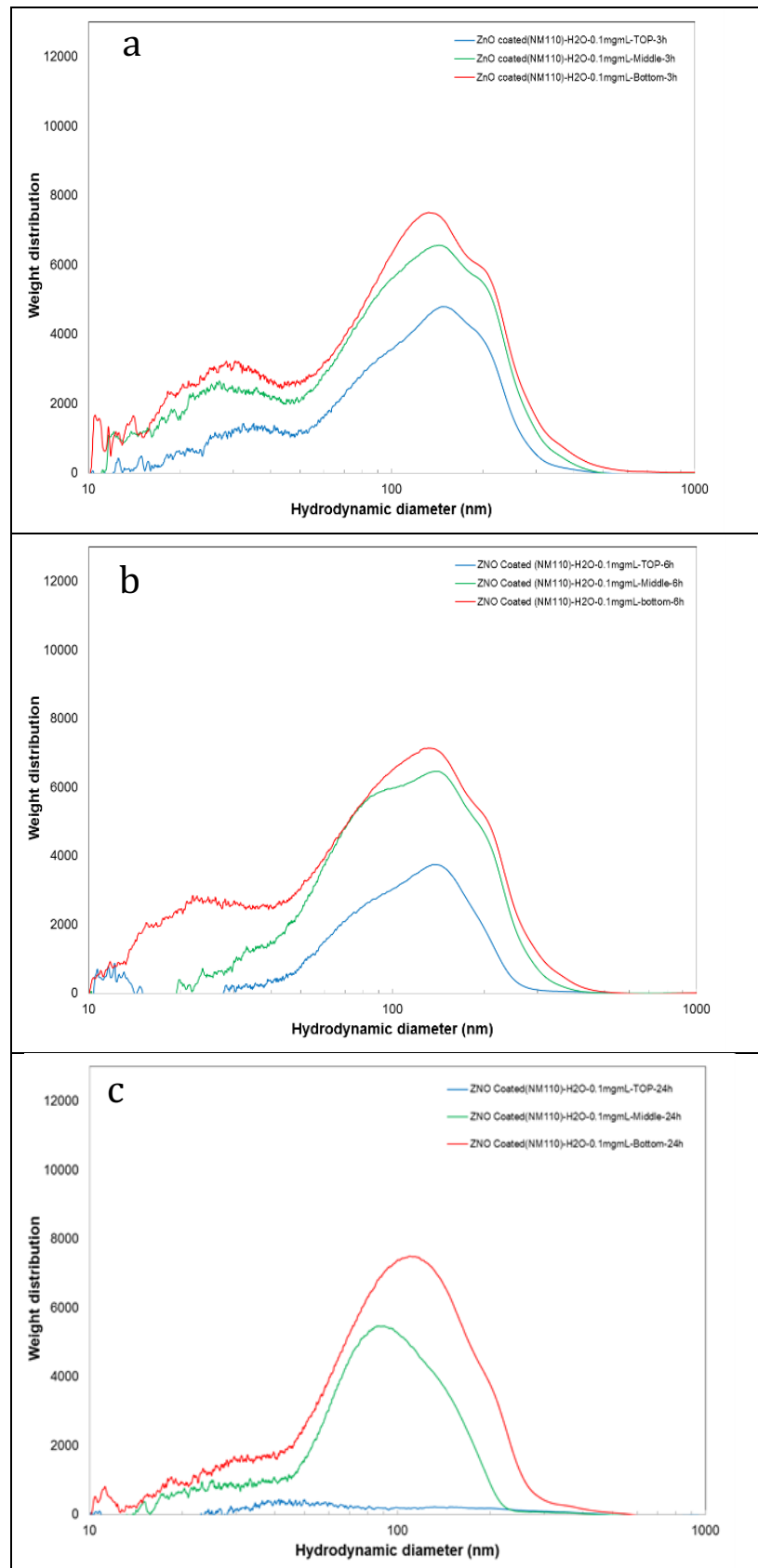


Figure 28: Particle size distribution of ZnO NM-111 in H<sub>2</sub>O (0.1 mg/mL) at different heights (Top, Middle and Bottom), with a fixed time a. 3h, b. 6h and c. 24h.

Diameters values of ZnO ENMs in M7 suspension (0.1mg/mL) over time and height, are reported in weight only and appear in **Table 24**. CLS spectra of these results are illustrated in Error! Reference source not found. and in Error! Reference source not found..

**Table 24: Diameter of primary particles (PP) and agglomerates (Agglo) of ZnO NM-111 suspended in M7 (0.1 mg/mL).**

Medium : Elendt M7 (0,1 mg/mL)		
TOP_Weight	Diameter PP (nm)	Diameter Agglo (nm)
0h	22.10	200
3h	35.50	190
6h	41.00	206
24h	30.50	221; 445
Middle_Weight		
0h	22.00	200
3h	42.00	147
6h	48.00	200
24h	27.00	224; 442
Bottom_Weight		
0h	22.00	200
3h	26.00	146; 207; 371
6h	27.00	155; 205; 368
24h	25.00	216; 438

In M7 medium, a different behaviour is observed. Over time, both populations of PP and Agglo decrease, in all the layers. After 3h, both are already found in the bottom of the vial. This observation indicates that ZnO ENMs seems to be less stable in M7 when compared to water and its sedimentation is faster. We have also noticed that for M7, in the bottom, the size of agglomerates changes with time (bimodal distribution becomes trimodal). In general, M7 medium and time seems to favour the agglomeration phenomenon.

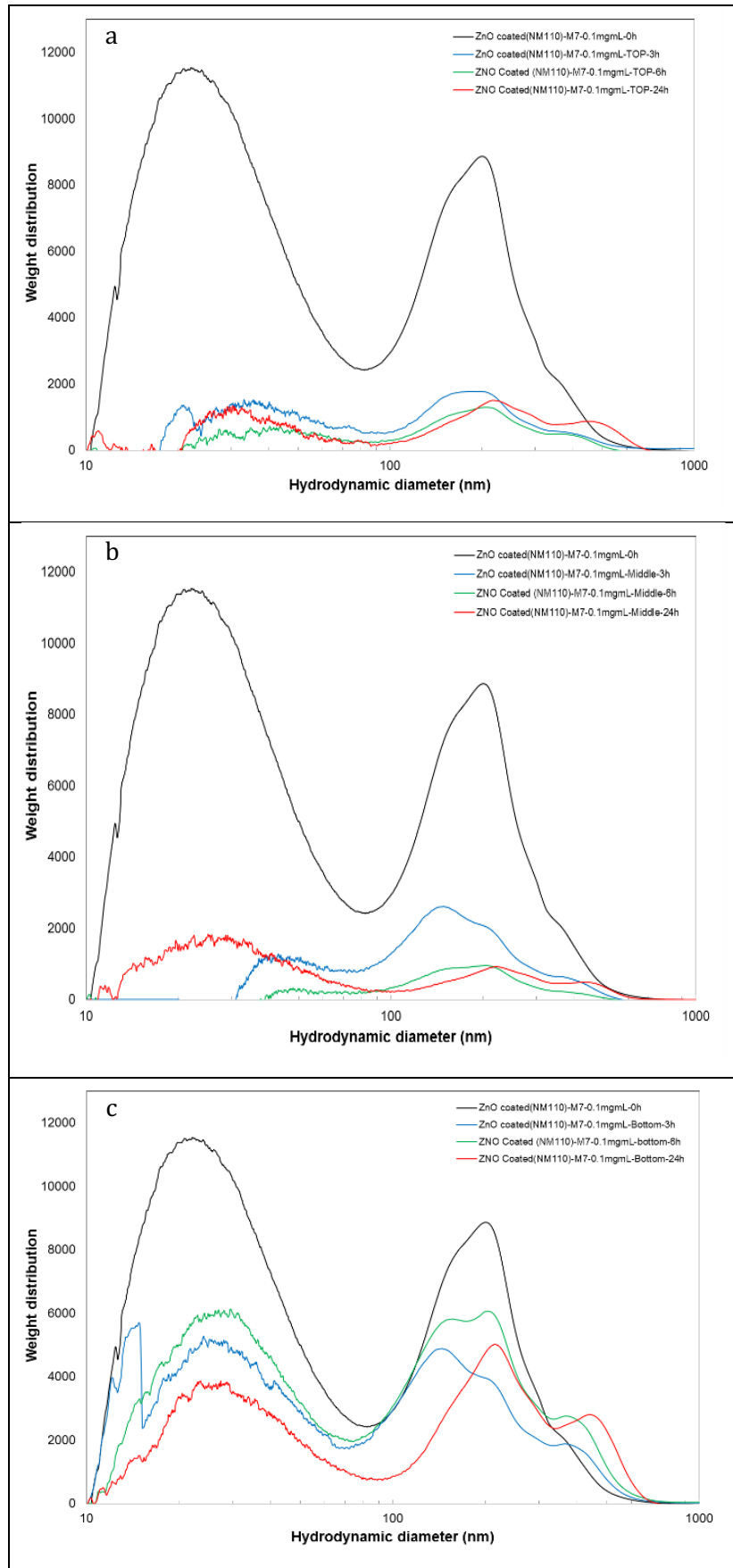


**Figure 29 : Particle size distribution of ZnO NM-111 in M7 (0.1 mg/mL) at different times (0, 3, 6 and 24h), with a fixed height a. Top, b. Middle and c. Bottom.**

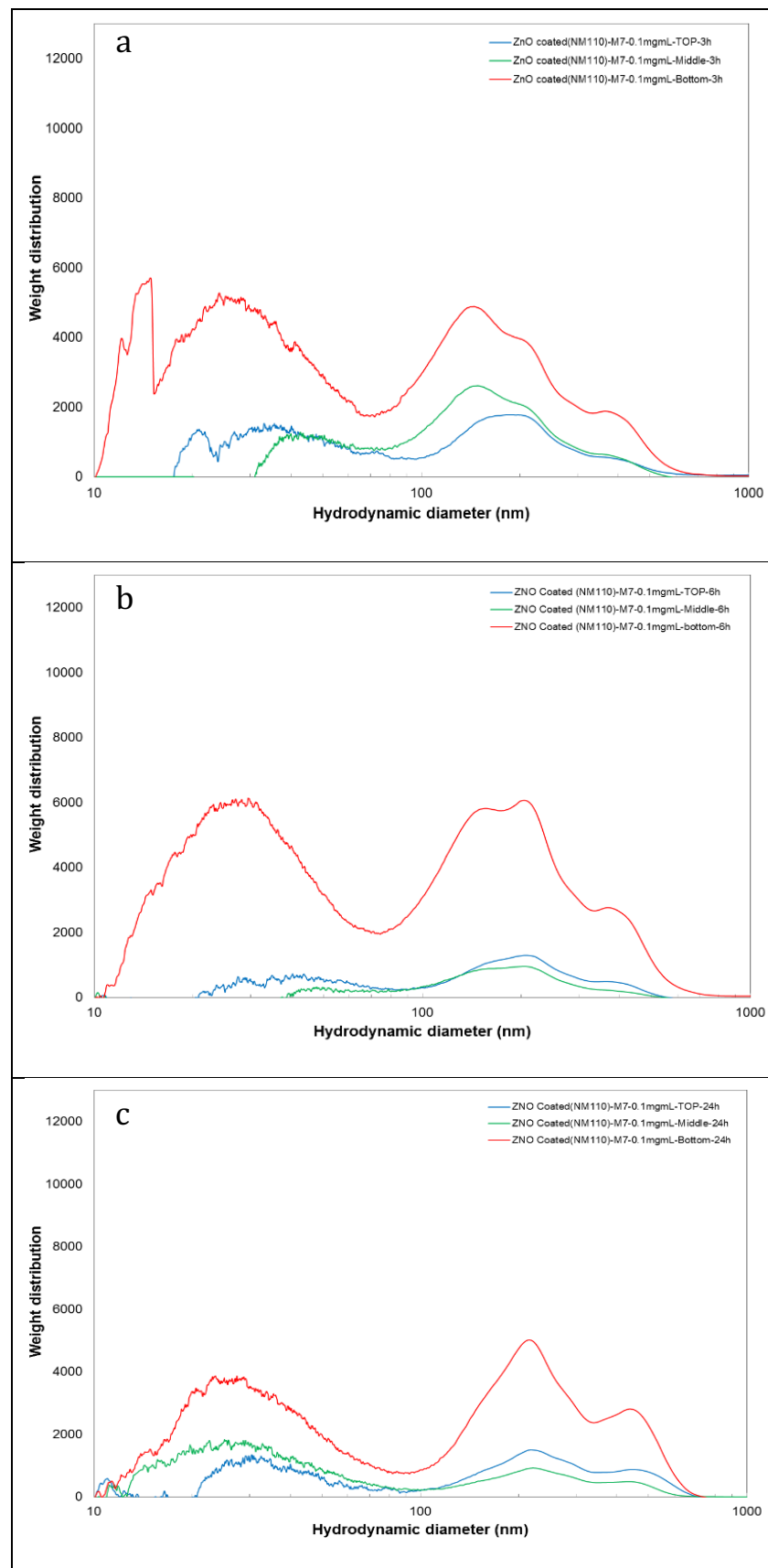


Figure 30 : Particle size distribution of ZnO NM-111 in M7 (0.1 mg/mL) at different heights (Top, Middle and Bottom), with a fixed time a. 3h, b. 6h and c. 24h.

To complete the experiment, pH was also measured at the beginning and after 24h of sedimentation. Values are listed in **Table 25**. pH tends to decrease slightly in H<sub>2</sub>O over time while in M7, the opposite is true. However, results are not sufficient to conclude that a modification in the pH takes place. This parameter seems to not be affected during the experiment in these conditions.

**Table 25: pH of ZnO NM-111 ENMs suspended in H<sub>2</sub>O and in M7, at the beginning of the experiment (0h) and after 24h of sedimentation.**

pH		H <sub>2</sub> O	M7
0h		8.213	7.886
24h	Top	7.398	8.025
	Middle	7.542	8.056
	Bottom	8.039	8.084

### **2.3.6 Fate assessment of nTiO<sub>2</sub> for long-term *Daphnia magna* tests**

The sedimentation process, agglomerate state and particle size distribution of TiO<sub>2</sub> NM-105 in suspension in *Daphnia* medium (Elendt M7) were studied with the CLS technique. The same protocol described in previous sections was used.

The NanoGENOTOX dispersion protocol and the SOP for calibration of Probe-sonicators for *in vitro* and *in vivo* testing were used for the suspension's preparation. In order to perform the experiment in more realistic conditions, low concentrations such as: 2, 5 and 10 mg/L were tested. A stock solution was prepared in water with a concentration of 100 mg/L and a final volume of 100 mL. It was sonicated for 10 min using a Branson Sonifer S-450D (Branson Ultrasonics, 300Watt, 10%Ampl, 13 mm horn). The analysed solution was prepared in Elendt M7 medium (preparation medium is based on OECD TG-211 (2012), OECD TG-202 (2004) and Elendt (1990), with minor modifications in methodology for practical reasons) with a concentration mentioned previously and a final volume of 50 mL. The suspension of 10mg/L, sampling was done at 4 different time: 0h, 2h, 24h and 48h and at 3 different height: Top (1.6 cm from the top), Middle (2.6 cm from the top) and Bottom (3.8 cm from the top). The dimensions of the vial are 2 cm\* 4 cm. For 5 mg/L, sampling was done only after 0 and 2h for the 3 positions while for 2 m/L, sampling was done at 0h. The experimental scheme appears in Error! Reference source not found..

### Sampling in CLS

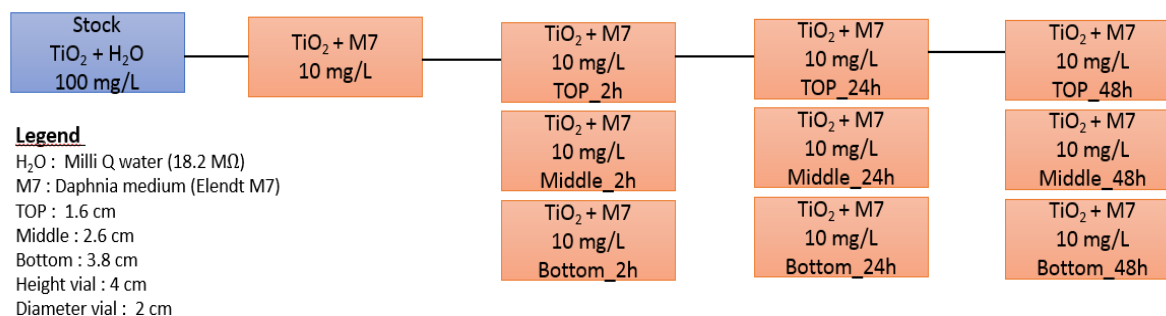


**Figure 31: Experimental scheme of the analysis of the particle size distribution by CLS of  $\text{TiO}_2$  NM-105 in M7 at different times (0, 2, 24 and 48h) and at different heights of the vial (Top, Middle and Bottom).**

Firstly, we analysed media to check if a background signal was produced in the CLS spectrum (**Figure 32**). Results indicate that almost no signal is detected for this media or  $\text{H}_2\text{O}$  or M7.

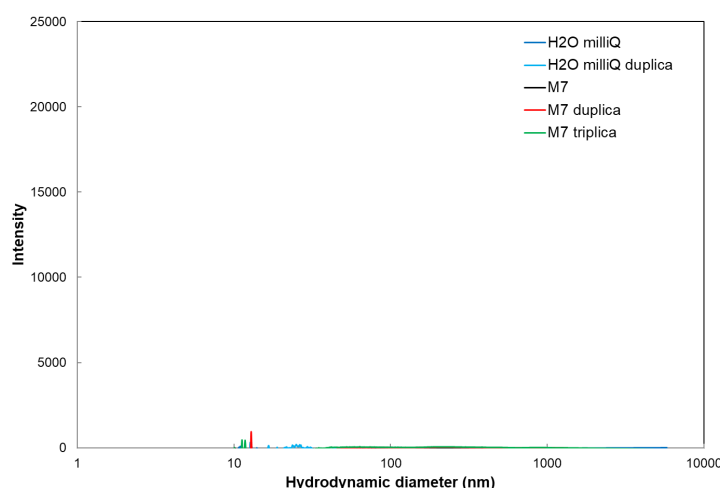


**Figure 32: Particle size distribution in weight by CLS of  $\text{H}_2\text{O}$  and M7.**

The stock solution analysed (Error! Reference source not found..a) shows two populations at 14.8 nm (PP) and at 72.1 nm (Agglo). Suspension of  $\text{TiO}_2$  NM-105 in M7, at a concentration of 2 mg/L, does not provide a reproducible particle size distribution (Error! Reference source not found..b). This low concentration is close to the limit of detection of the instrument.

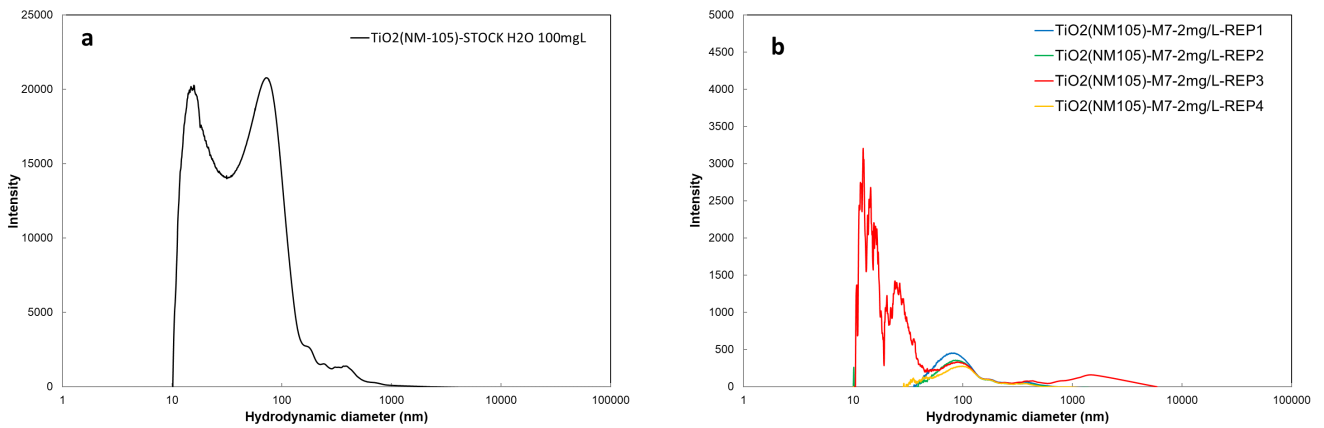


**Figure 33: Particle size distribution of TiO<sub>2</sub> NM-105 in a. H<sub>2</sub>O (100 mg/L), and in b. M7 (2mg/L) at 0h (4 replicates).**

Stock solution (Error! Reference source not found.. a) shows 2 populations at 18 nm (PP) and at 109.1 nm (Agglo). At a concentration of 5 mg/L (Error! Reference source not found.. b), only a peak corresponding to primary particles is observed. However, repeatability with triplicates was not achieved (**Error! Reference source not found..c**). Once again, the concentrations analysed were close to the instrument LOD.

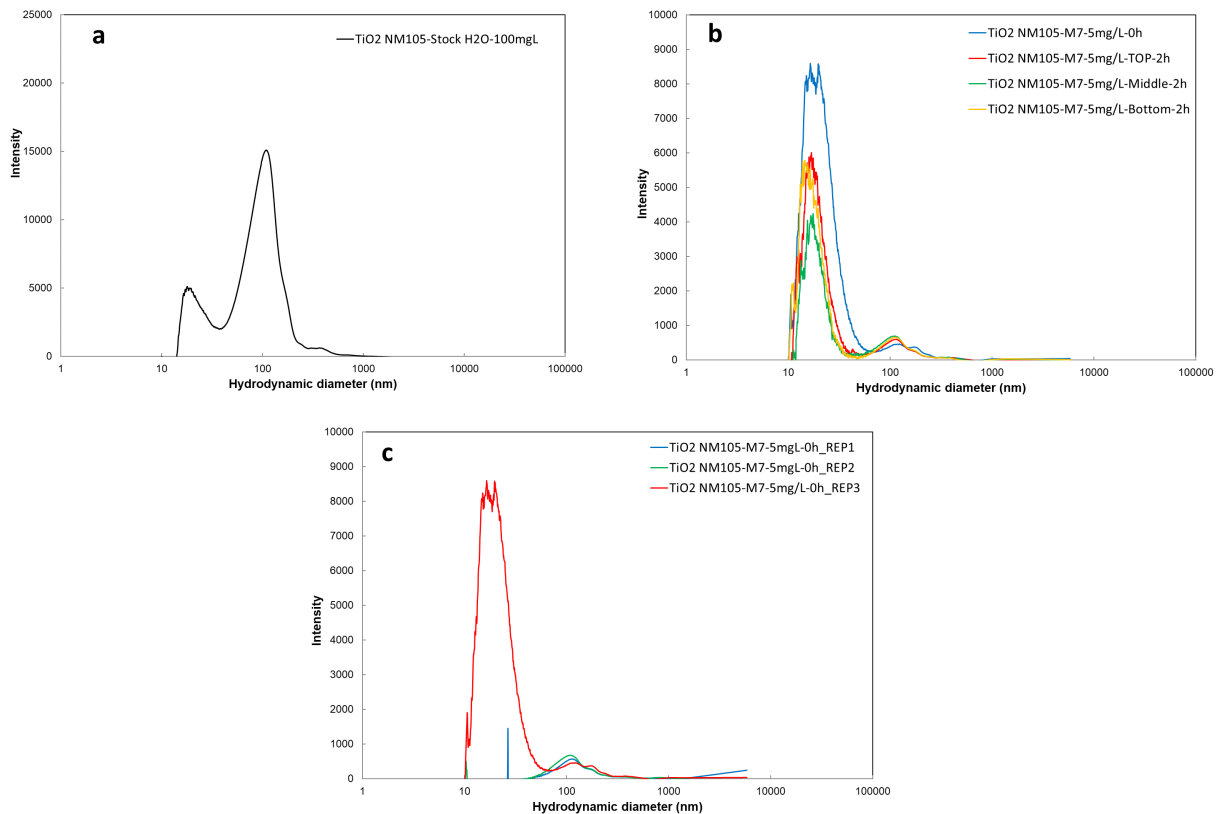


**Figure 34: Particle size distribution of TiO<sub>2</sub> NM-105 in a. H<sub>2</sub>O (100 mg/L), b. M7 (5 mg/L) at 0h and 2h at different heights (Top, Middle and Bottom), c. M7 (5 mg/L) at 0h in triplicate.**

At a concentration of 10 mg/L, more reproducibility is achieved. A sedimentation process was observed for most samples. We noticed that results after 24 h of sedimentation are similar to those at 48h. The stock solution (**Figure .a**) shows 2 populations of particles at 12 nm (PP) and at 112.4 nm (Agglo). A dilution in medium M7 to achieve 10 mg/L, modifies the population of agglomerates (**Figure .b**), three populations appear at 128.7, 183.5 and 233.7 nm. After 24h, in the Top point (**Figure .b**), all the agglomerates have sedimented towards the lower layers. In the middle section (**Figure .c**), agglomerates remain unchanged after 2h but after 24h, all have sedimented. At the bottom section (**Figure .d**), agglomerates remain present even after 48h (formation of a sediment).

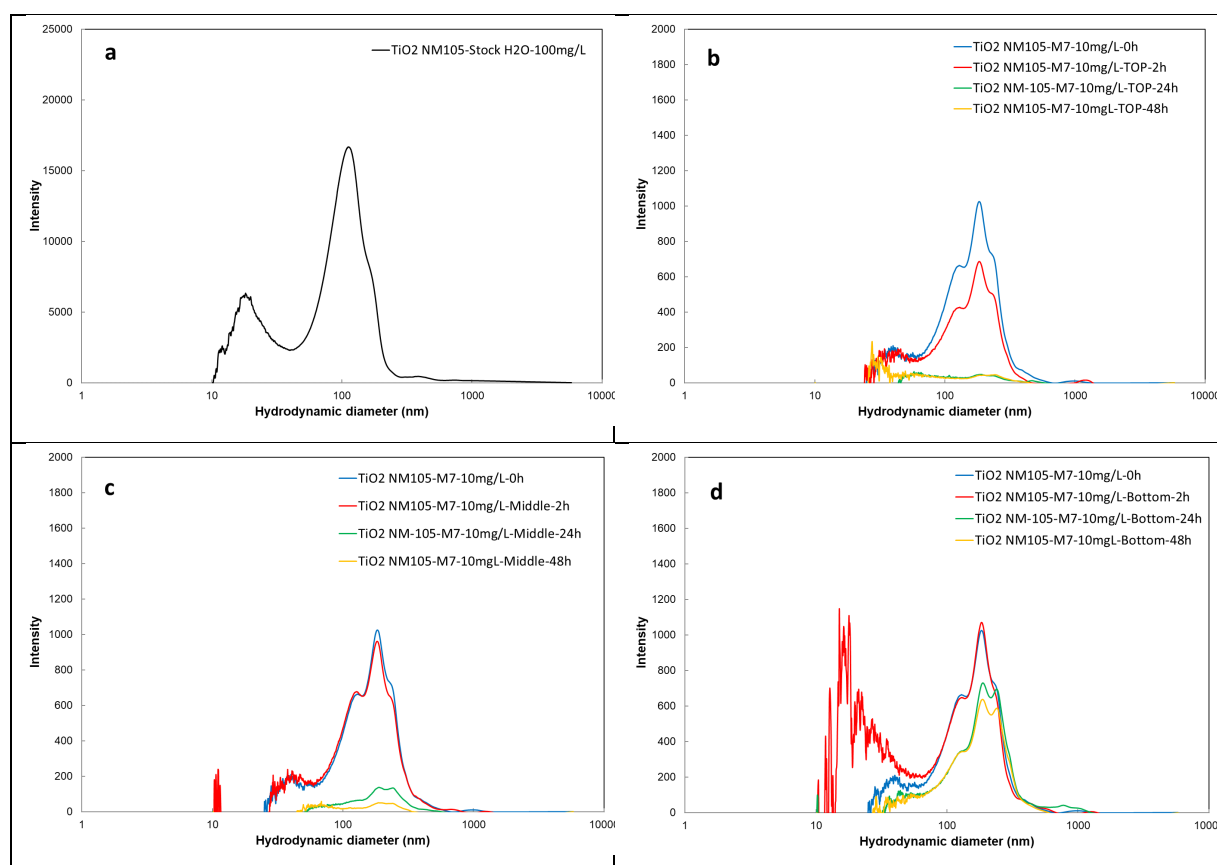


**Figure 35 : Particle size distribution of TiO<sub>2</sub> NM-105 in a. H<sub>2</sub>O (100 mg/L), b. M7 (5 mg/L) at 0, 2, 24 and 48h at the Top, c. M7 (5 mg/L) at 0, 2, 24 and 48h at the Middle, d. M7 (5 mg/L) at 0, 2, 24 and 48h at the Bottom.**

### **2.3.7 Fate assessment of nTiO<sub>2</sub> for long-term Egg water tests**

Sedimentation process, agglomerate state and particle size distribution of TiO<sub>2</sub> NM-105 in suspension in Egg water, were studied with the CLS technique. For this study the same CLS

methodology and the NanoGENOTOX dispersion protocol was used as described in previous sections.

Suspensions of 5 and 10 mg/L were prepared in Egg water at 60 mg/L. The Egg water solution was prepared from Instant Ocean Salts supplied by partners. A stock solution of Instant Ocean Salts 6 g/L was prepared and was diluted 100 times to obtain Egg water at 60 mg/L.

Sampling was done at 4 different times: 0h, 2h, 24h and 48h and at 3 different heights: Top (1.6 cm from the top), Middle (2.6 cm from the top) and Bottom (3.8 cm from the top). The dimensions of the vial are 2 cm\* 4 cm. The experimental scheme is shown in **Figure** .

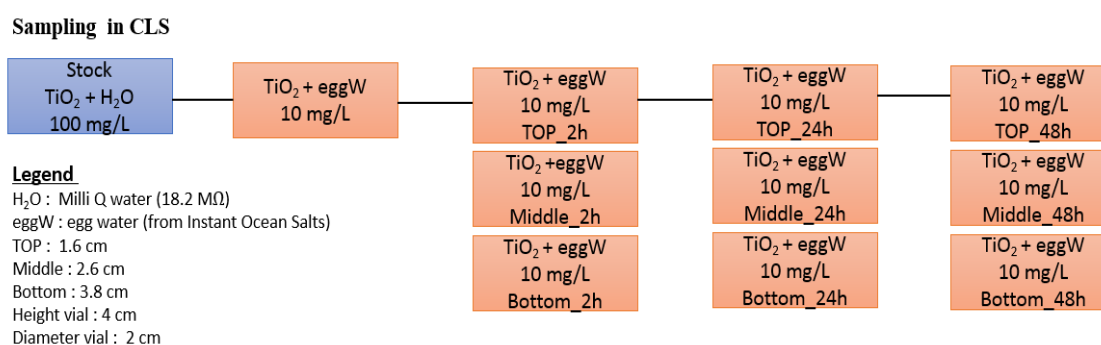


**Figure 36 : Experimental scheme of the particle size distribution analysis by CLS of TiO<sub>2</sub> NM-105 in Egg water at different times (0, 2, 24 and 48h) and at different heights of the vial (Top, Middle and Bottom).**

At a concentration of 5 mg/L (**Figure** ), TiO<sub>2</sub> NPs in stock solution 100mg/L, show a quasi bi-modal distribution with one peak located at 13 nm and another peak at 65 nm (**Figure .a**). On the top, middle and bottom of the vial, only agglomerates are detected. A small signal of PP is observed near 13 nm, but the concentration was too low to detect a real signal for PP (**Figure . b,c,d**).

At a concentration of 10 mg/L (**Figure** ), TiO<sub>2</sub> NPs in stock solution 100mg/L, show a bi-modal distribution with one peak located at 12 nm and another peak at 107 nm (**Figure .a**). The concentration of 10 mg/L allows a better resolution for the peaks detected. This means that 5 mg/L is close to the limit of detection. At the top, after 2h, PP and agglomerates are observed but after 24h and 48h, all has sedimented in the lower layers (**Figure .b**). In the middle, after 2h, PP cannot be detected as only agglomerates are observed. After 24h and 48h, agglomerates were dropping down (**Figure .c**). In the bottom, agglomerates are observed even after 2h (**Figure .d**).

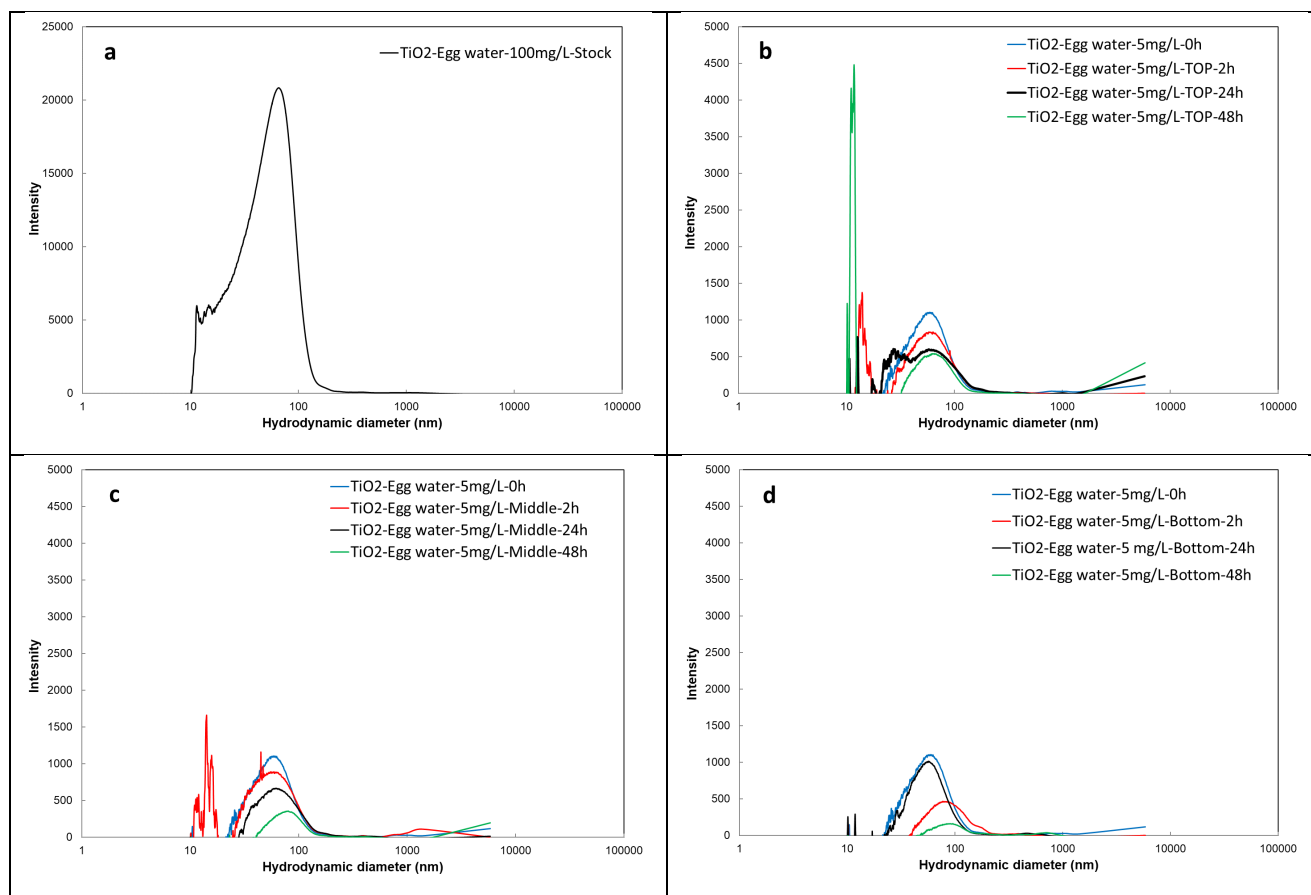


**Figure 37 : Particle size distribution of TiO<sub>2</sub> NM-105 in a. H<sub>2</sub>O (100 mg/L), b. Egg water (5 mg/L) at 0, 2, 24 and 48h at the Top, c. Egg water (5 mg/L) at 0, 2, 24 and 48h at the Middle, d. Egg water (5 mg/L) at 0, 2, 24 and 48h at the Bottom.**

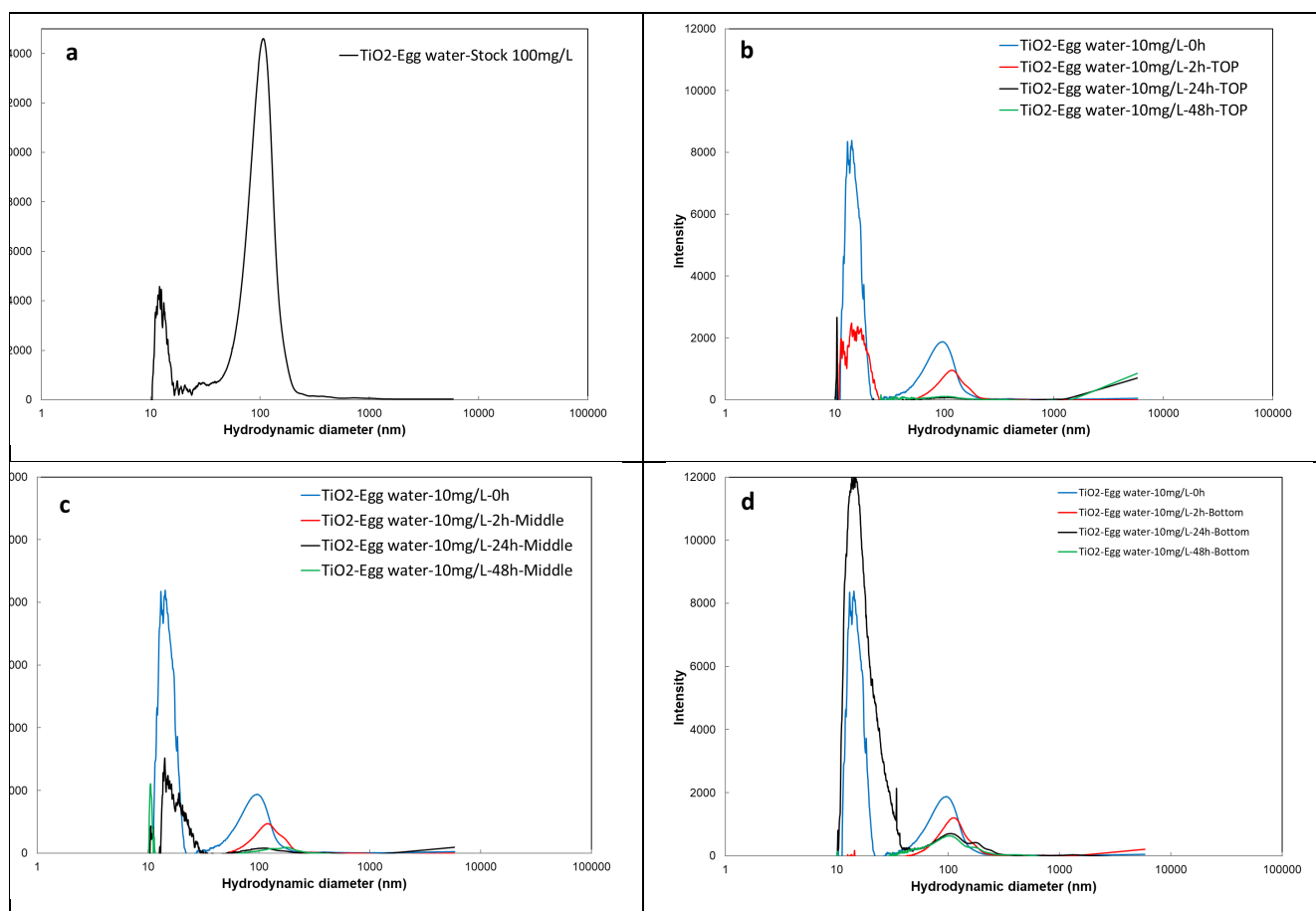


**Figure 38: Particle size distribution of TiO<sub>2</sub> NM-105 in a. H<sub>2</sub>O (100 mg/L), b. Egg water (10 mg/L) at 0, 2, 24 and 48h at the Top, c. Egg water (10 mg/L) at 0, 2, 24 and 48h at the Middle, d. Egg water (10 mg/L) at 0, 2, 24 and 48h at the Bottom.**

The sedimentation studies highlight that the behaviour of ENMs is related to the ecotox media. For example, ZnO sediment faster in water only with respect to M7. TiO<sub>2</sub> sediment faster in Egg water while the contrary happens in M7 medium. Overall, these results suggest that particle size determinations must be evaluated during ecotox experiments.

### 2.3.8 Characterisation of Zebra fish eggs exposed to NPs

In collaboration with UL (WP5), some sets of samples from zebrafish eggs were analysed by the Particle Induced X-ray Emission (PIXE) technique. Samples were first lyophilised before transfer to the UNamur. Later, the samples were placed on top of a substrate and fixed using milliQ water. Different substrates, to place the sample on top, were used: Al, C and recently Au coating on carbon. This layer is later used to define the substrate depth, which is a parameter during the sample analysis. The methodology used was the one established previously in the NanoReg project. Most of the samples were concentrated via several steps of evaporation (Air pulsed oven at 70°C) to have concentrations higher than the LOD of the

technique. However, several improvements, to gain in quality of the samples and the results, were and continue to be realised. The principal drawbacks are the small sample quantity and the lower concentrations.

**Figure 39** shows the Ti concentration in Zebrafish eggs exposed to different concentrations of TiO<sub>2</sub> NPs (theoretical medium concentrations of 2, 5 and 10 mg/L). The concentrations observed follow the same trends of the theoretical exposure concentrations.

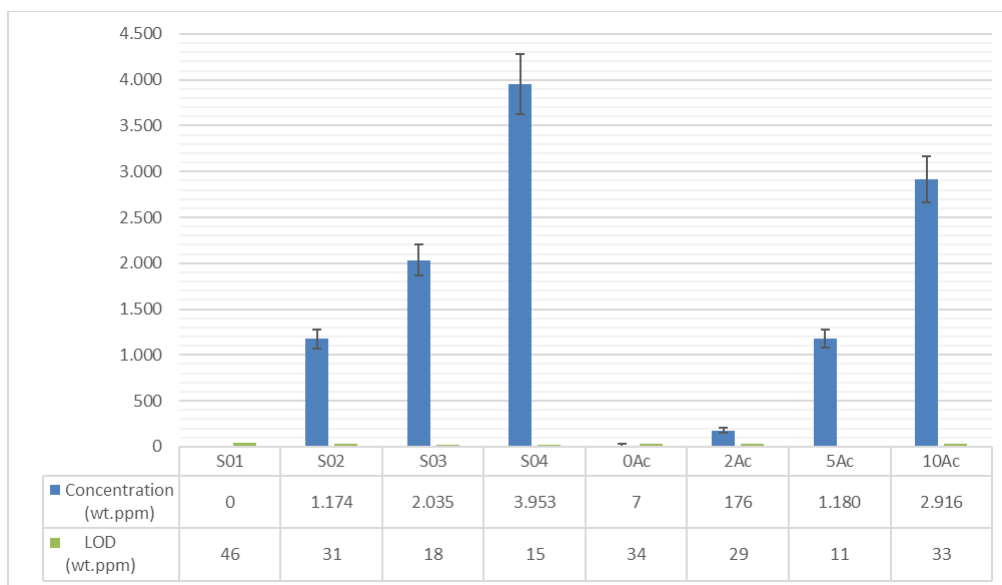


**Figure 39: Evolution of the Ti concentration in Zebrafish eggs exposed to TiO<sub>2</sub> NPs measured by PIXE (LOD: Limit Of Detection).**

Error! Reference source not found. shows the variation of all the elements composing the sample (matrix). Variations in Cl and K seems to follow the Ti trend.

This data can potentially be used as validation for the matrix modifications, for dosimetry models. Lower concentrations, sub ppm, are still a challenge for the PIXE technique, therefore sampling concentration is a frontline subject. Next to this, the possibility to trace potential changes in the matrix, due to the presence of certain NPs aside from the principal effects, is an aspect that merits further exploration.

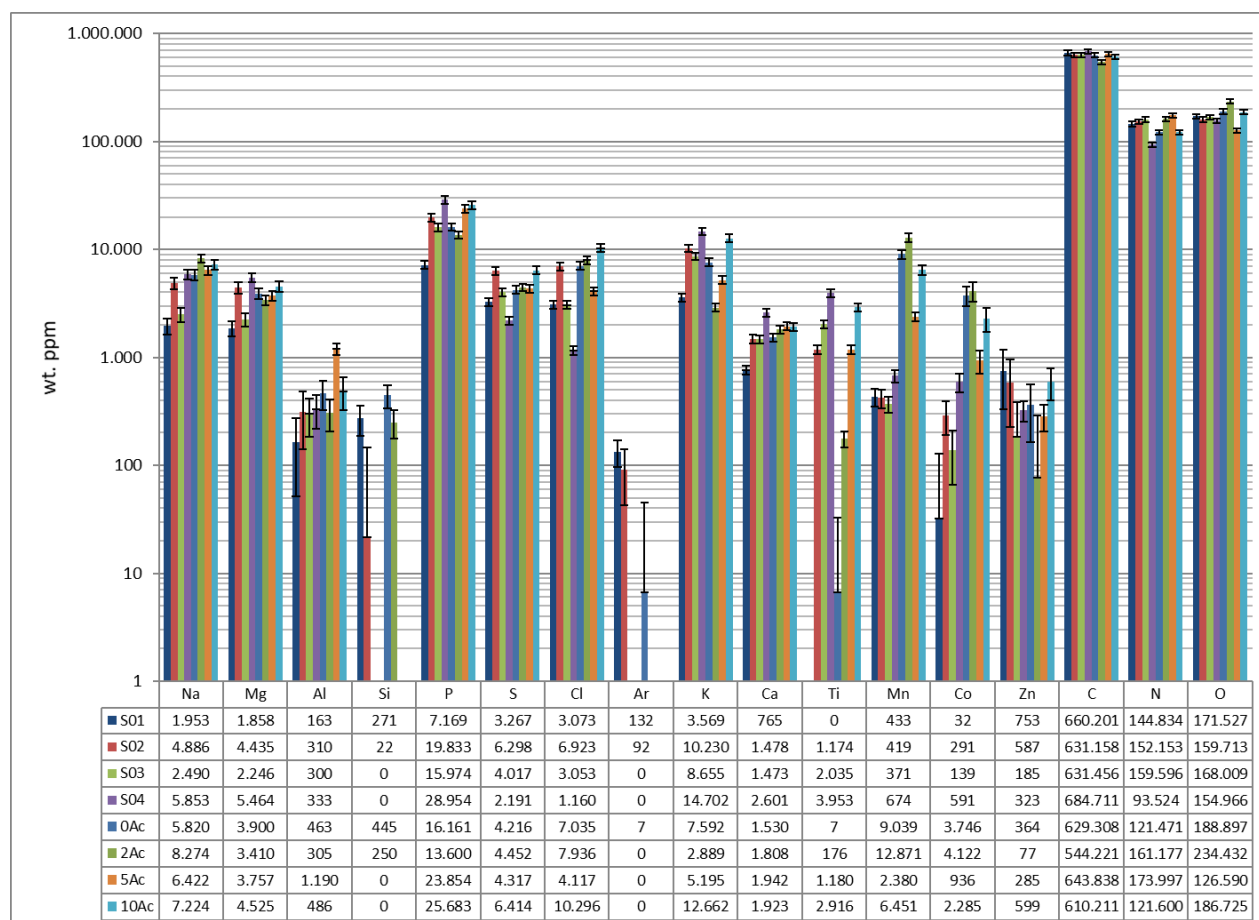


Figure 40: Evolution of the elements concentration in Zebrafish eggs exposed to TiO<sub>2</sub> NPs measured by PIXE (LOD: Limit Of Detection).

Some other set of experiments were conducted on Zebrafish eggs that were treated/fixated with or without PFA. The main results are shown in Figure 41.

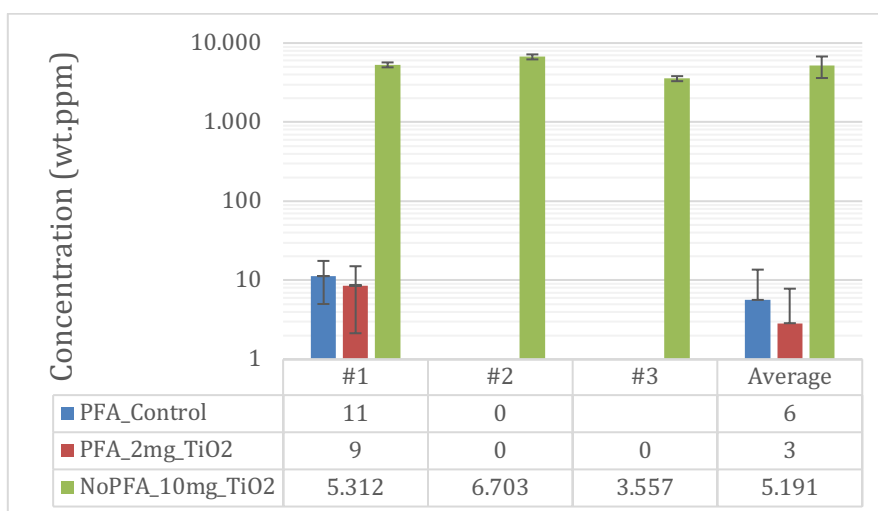
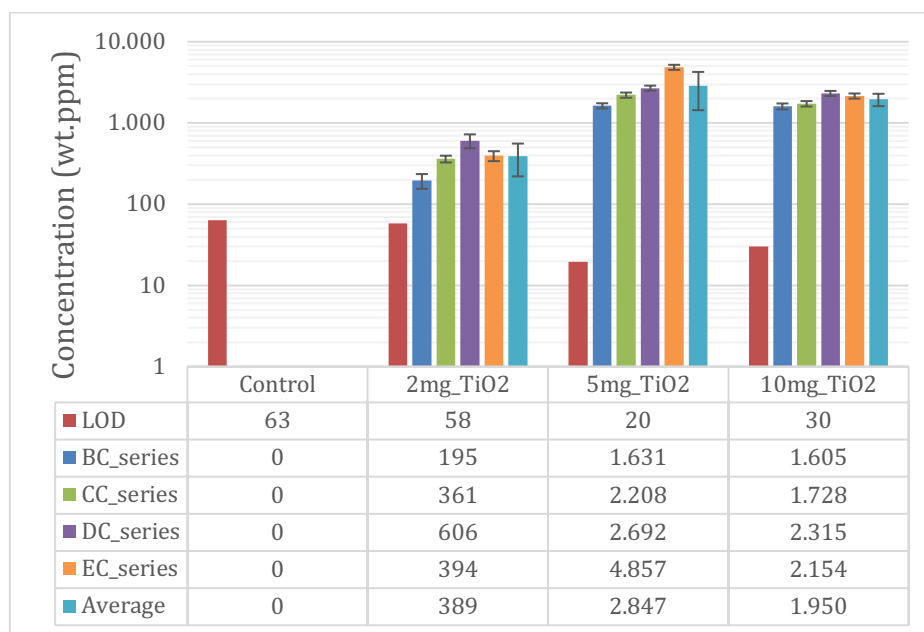


Figure 41: Evolution of the concentration in Zebrafish eggs exposed to a concentration of 2 mg/mL TiO<sub>2</sub> NPs, with PFA fixation, measured by PIXE.

In this experiment, the objective was to highlight if the PFA mixing method influences the sorption of TiO<sub>2</sub> NPs in the chorion of Zebrafish. The different series are presented in **Figure 42** measured at 2, 5 and 10 mg of TiO<sub>2</sub>.



**Figure 42: Evolution of the concentration in Zebrafish eggs exposed to different concentrations of TiO<sub>2</sub> NPs, with and without PFA, measured by PIXE.**

PFA leads to serious issues in terms of X-ray detection due to the concentrations of Na and Cl. Those concentrations are much higher for the samples with PFA (~100 000 wt.ppm) compared to samples without PFA (~5 000 wt.ppm). Those very intense peaks lead to a large pile-up effect, that falls in the 4 – 6 keV range, which corresponds to the Ti signal (K<sub>a</sub> = 4.51 keV & K<sub>b</sub> = 4.93 keV). As a direct consequence, the LOD for Ti jumps from about 30 wt.ppm for samples without PFA to about 350 wt.ppm for samples containing PFA. Consequently, no Ti has been measured for the control and 2 mg/ml samples containing PFA (i.e. [Ti] < 350 wt.ppm).

For the 10 mg/ml sample, we found an average of  $(5.2 \pm 1.6) \times 10^3$  wt.ppm for the Ti concentration, or  $(8.7 \pm 2.6) \times 10^3$  wt.ppm for the Ti concentration. This concentration is significantly higher than the one found for the BC – EC series samples at the same concentration:  $(1.9 \pm 0.3) \times 10^3$  wt.ppm for the Ti concentration, or  $(3.2 \pm 0.6) \times 10^3$  wt.ppm for the Ti concentration.

Increasing the concentration of TiO<sub>2</sub> in the medium from 2 to 5 mg/ml leads to an increase of the TiO<sub>2</sub> NPs uptake by Zebrafish eggs. However, it seems that the uptake process reaches saturation since no further increase of Ti concentration measured by PIXE is observed when

the TiO<sub>2</sub> concentration in the medium is increased from 5 to 10 mg/ml. These results were evaluated in WP5 and they will be part of a peer review paper.

### **2.3.9 Overall conclusions**

Task 1.5 was devoted to produce data on the Environmental fate and dosimetry of Tier 1 ENMs. A first step towards this objective was to characterise ENMs in relevant ecotox media, such as: Egg water and M7. Several sets of data were produced, with different techniques (BET, XPS, TEM, CLS, DLS, ELS). This data highlights the interaction between the ENMs and the ecotox relevant media where they are dispersed.

Later, the ENMs fate in the water column was evaluated based on sedimentation, size, zeta potential and colloidal stability studies. Principal findings reveal that ENMs fate is dependent on the ecotox media. There is a correlation between NPs agglomeration and time of exposure. Furthermore, a new set-up was optimised and validated to estimate the concentration of ENMs at half water column height and to evaluate the sedimentation rate in a typical *in vivo* model.

The sedimentation studies highlight that the ENMs behavior is related to the ecotox media. For example, ZnO sediment faster in water with respect to M7. TiO<sub>2</sub> sediment faster in Egg water while the contrary is true in M7 medium. Overall, these results suggest that particle size and sedimentation behaviors determinations must be evaluated during ecotox experiments.

### **3. Deviations from the Workplan**

WP5 provided two different media to WP1 for the acute ENM exposure assays using daphnia and zebrafish embryo-larve: M7 for daphnia and Egg Water for zebrafish. To minimise the potential influences on ENM suspension by transport and other external factors, all ENM suspensions for the analyses were prepared at the sites of the WP1 team. WP5 were provided with the results of particle size measurement using DLS for three different concentration of CeO<sub>2</sub>NP and ZnONPs, measured at 1 hour and 24 hours after the preparation of the solutions in these two media (also 72 hours for ZnO in M7 media). The data indicated very large particle sizes in the ENM suspensions, ranging from a few µm to over 10µm diameter under all experimental conditions. These results suggest that a significant degree of aggregation in the tested ENM suspensions may have occurred. WP5 also obtained the dissolution kinetics data of ZnONP (coated or non-coated) and total Ti measurements from a series of TiO<sub>2</sub>NP dilutions using ICP-OES5100 from WP1. However, those measurements were limited to daphnia media and not conducted for zebrafish media.

It was not clear why there were such high levels of aggregation in the test media, but it may have been related to a problem in maintaining the media qualities during the shipping from WP5 to WP1 sites. WP5 thus took alternative approaches to obtain the fate and dosimetry data for ENM suspensions by conducting the measurements at their own sites (UL, DTU) or in a local collaborator's laboratory (UNEXE). Each WP5 team has finished (except for HWU who is still waiting for the results from WP1) the measurements for the specific ENMs that have been chosen to test for the acute ENM exposure bioassays in different model animals and different media (please see **"2. Description of work & main achievements"** for the achievements by UNEXE).

Although WP1 and WP5 partners have collaboratively worked as originally planned in WP1.5, high quality data were not obtained for the fate and dosimetry analyses for ENM suspensions in exposure media. Alternative approaches were therefore taken to conduct these assays on site or at a local collaborator's laboratory. UNEXE have completed the fate analyses of Ag NPs and ZnO NPs suspensions which induce oxidative stress responses in specific tissues (WP5.2 deliverable). The results obtained led to further characterisation of the mode of action of each metal NP in acute exposures.

UNamur used the PIXE technique to evaluate the concentration of ENMs in different media after several types of experiences, with samples produced in house or provided by different partners (WP1/WP5). The low concentration used for the experiments, with respect to previous nanosafety projects, demanded modifications in the original setup. For example, the sample holder was modified several times in order to improve the measurement capabilities (lower sample volume). Analysis, either on liquid or dried samples, were evaluated to choose the best conditions to produce the most reliable results. These modifications were more challenging and more time consuming than expected. For this reason, the number of samples analysed was lower than estimated in the original planning.

The Covid-19 confinement, which for most institutions took place from mid-March to mid-June, had an impact on the remaining experiments. Experiments and data treatment planned between this period were delayed.

The decision of the PATROLS Steering Board to postpone the deliverables with deadlines closed to the period mentioned before, set the conditions to accomplish most of the pending experiments. In the case of the UNamur, experiments were planned with the  $\mu$ PIXE technique, which would have complemented local identification (mapping) of agglomerates of NPs on the tested samples. However, this experiment could not be performed due to a delay with expected

parts required for the setup (before the calibration of the system) or parts required to run samples such as those from PATROLS (lower concentrations and lower volumes). Nonetheless, the objectives related to this deliverable were not considerably affected by this situation given that relevant ecotox data was produced with the PIXE technique.

#### 4. Performance of the partners

T1.5 partners worked in close collaboration to achieve most of the objectives of this deliverable. At the beginning there was a high demand on physicochemical characterisation data to properly initiate experiments in other WPs (WP5 especially). These demands, were fulfilled in the best manner. However, not all of them were satisfied, given the time required for such experiments and that most of them were not originally described in the Grant Agreement. As a consequence, the original planning was rearranged, which produced some delays in further planned activities for some partners.

Partners, such as ISTECH, contributed to Task 1.5 whereas it was not originally in their responsibilities. Partner BASF, contributed less to D1.5 and more to T1.2 than originally described in the Grant Agreement as objectives were slightly redefined. Overall, all partners have participated in a productive and collaborative way.

#### 5. Conclusions

The Steering Board deems this deliverable to be satisfactorily fulfilled for submission

#### 6. Annex - References

1. Rasmussen, K.; Mast, J.; De Temmerman, P.-J.; Verleysen, E.; Waegeneers, N.; Van Steen, F.; Pizzolon, J. C.; De Temmerman, L.; Van Doren, E.; Jensen, K. A., Titanium dioxide, NM-100, NM-101, NM-102, NM-103, NM-104, NM-105: characterisation and physico-chemical properties. *JRC science and policy reports* **2014**.
2. Rasmussen, K.; Mech, A.; Mast, J.; De Temmerman, P.; Waegeneers, N.; Van Steen, F.; Pizzolon, J.; De Temmerman, L.; Van Doren, E.; Jensen, K. A., Synthetic Amorphous Silicon Dioxide (NM-200, NM-201, NM-202, NM-203, NM-204). Characterisation and Physico-Chemical Properties. *JRC Scientific and Policy Reports* **2013**.

3. Singh, C.; Friedrichs, S.; Levin, M.; Birkedal, R.; Jensen, K.; Pojana, G.; Wohlleben, W.; Schulte, S.; Wiench, K.; Turney, T., Zinc Oxide NM-110, NM-111, NM-112, NM-113: Characterisation and Test Item Preparation In: NM-Series of Representative Manufactured Nanomaterials. *Ispra, Italy: Joint Research Centre of the European Commission* **2011**.
4. Rasmussen, K.; Mast, J.; De Temmerman, P.; Verleysen, E.; Waegeneers, N.; Van Steen, F., Multi-walled Carbon Nanotubes, NM-400, NM-401, NM-402, NM-403: Characterisation and Physico-Chemical Properties. European commission; 2014. Report No.: 26796. 2018.
5. Synthetic amorphous silicon dioxide (NM-200, NM-201, NM-202, NM-203, NM-204). Characterisation and physico-chemical properties : JRC repository : NM-series of representative manufactured nanomaterials. European Commission, Joint Research Centre, Institute for Health and Consumer Protection. ISBN 978-92-79-32323-2. 2013
6. Effects of the dispersion methods in Pluronic F108 on the size and the surface composition of MWCNTs and their implications in toxicology assessment. Mejia, J., Mekhalif, Z., Delhalle, J., Lucas, S., Tichelaar, F., Saout, C., Toussaint, O. & Masereel, B., 2011, *Journal of Nanoparticle Research*. 13, 2, p. 655-667 13 p.
7. NM-Series of Representative Manufactured Nanomaterials - Zinc Oxide NM-110, NM-111, NM-112, NM-113: Characterisation and Test Item Preparation. European Commission, Joint Research Centre, Institute for Health and Consumer Protection. ISBN: 978-92-79-22215-3. 2011
8. DeLoid, G.; Cohen, J. M.; Darrah, T.; Derk, R.; Rojanasakul, L.; Pyrgiotakis, G.; Wohlleben, W.; Demokritou, P., Estimating the effective density of engineered nanomaterials for in vitro dosimetry. *Nature communications* **2014**, 5, 3514.
9. DeLoid, G. M.; Cohen, J. M.; Pyrgiotakis, G.; Pirela, S. V.; Pal, A.; Liu, J.; Srebric, J.; Demokritou, P., Advanced computational modeling for in vitro nanomaterial dosimetry. *Particle and fibre toxicology* **2015**, 12 (1), 32.
10. DeLoid, G. M.; Cohen, J. M.; Pyrgiotakis, G.; Demokritou, P., Preparation, characterisation, and in vitro dosimetry of dispersed, engineered nanomaterials. *Nature protocols* **2017**, 12 (2), 355.
11. Pal, A. K.; Bello, D.; Cohen, J.; Demokritou, P., Implications of in vitro dosimetry on toxicological ranking of low aspect ratio engineered nanomaterials. *Nanotoxicology* **2015**, 9 (7), 871-885.
12. Watson, C.; DeLoid, G.; Pal, A.; Demokritou, P., Buoyant Nanoparticles: Implications for Nano-Biointeractions in Cellular Studies. *Small* **2016**, 12 (23), 3172-3180.
13. ECHA Appendix R. 6-1: Recommendations for nanomaterials applicable to the Guidance on QSARs and Grouping. **2017**, 29, doi:10.2823/884050.

14. Mitrano, D.M.; Motellier, S.; Clavaguera, S.; Nowack, B. Review of nanomaterial aging and transformations through the life cycle of nano-enhanced products. *Environ. Int.* **2015**, *77*, 132–147, doi:10.1016/J.ENVINT.2015.01.013.
  15. Häder, D.-P.; Erzinger, G.S. OECD Guidelines for testing of chemicals. **1998**, 1–21, doi:10.1016/B978-0-12-811861-0.00011-5.
  16. Samel, A.; Ziegenfuss, M.; Goulden, C.E.; Banks, S.; Baer, K.N. Culturing and Bioassay Testing of *Daphnia magna* Using Elendt M4, Elendt M7, and COMBO Media. *Ecotoxicol. Environ. Saf.* **1999**, *43*, 103–110, doi:10.1006/EESA.1999.1777. Kallay, N.; Kovačević, D.; Žalac, S. Thermodynamics of the solid/liquid interface - its application to adsorption and colloid stability. *Interface Sci. Technol.* **2006**, *11*, 133–170, doi:10.1016/S1573-4285(06)80050-5.
  17. Fatehah, M.O.; Aziz, H.A.; Stoll, S. Stability of ZnO Nanoparticles in Solution. Influence of pH, Dissolution, Aggregation and Disaggregation Effects. *J. Colloid Sci. Biotechnol.* **2014**, *3*, 75–84, doi:10.1166/jcsb.2014.1072.
  18. Degen, A.; Kosec, M. Effect of pH and impurities on the surface charge of zinc oxide in aqueous solution. *J. Eur. Ceram. Soc.* **2000**, *20*, 667–673, doi:10.1016/S0955-2219(99)00203-4.
  19. Dahirel, V.; Jardat, M. Effective interactions between charged nanoparticles in water: What is left from the DLVO theory? *Curr. Opin. Colloid Interface Sci.* **2010**, *15*, 2–7, doi:10.1016/J.COCIS.2009.05.006.
  20. Rasmussen, K.; Mast, J.; Temmerman, P. De; Verleysen, E.; Waegeneers, N.; Steen, F. Van; Pizzolon, J.C.; Temmerman, L. De; Van, E.; Jensen, K.A.; et al. *Titanium Dioxide, NM-100, NM-101, NM-102, NM-103, NM-104, NM-105: Characterisation and Physico- Chemical Properties*; 2014; ISBN 9789279381881.
  21. Lolli, A.; Blosi, M.; Ortelli, S.; Costa, A.L.; Zaroni, I.; Bonincontro, D.; Carella, F.; Albonetti, S. Innovative synthesis of nanostructured composite materials by a spray-freeze drying process: Efficient catalysts and photocatalysts preparation. *Catal. Today* **2019**, *334*, 193–202, doi:10.1016/j.cattod.2018.11.022.
  22. Holmberg, J.P.; Ahlberg, E.; Bergenholtz, J.; Hassellöv, M.; Abbas, Z. Surface charge and interfacial potential of titanium dioxide nanoparticles: Experimental and theoretical investigations. *J. Colloid Interface Sci.* **2013**, *407*, 168–176, doi:10.1016/J.JCIS.2013.06.015.
  23. Häder, D.-P.; Erzinger, G.S. OECD Guidelines for testing of chemicals - *Daphnia magna* Reproduction Test. *OECD* **1998**, 1–21, doi:10.1016/B978-0-12-811861-0.00011-5.
  24. Samel, A.; Ziegenfuss, M.; Goulden, C.E.; Banks, S.; Baer, K.N. Culturing and Bioassay Testing of *Daphnia magna* Using Elendt M4, Elendt M7, and COMBO Media.
-

- Ecotoxicol. Environ. Saf.* **1999**, *43*, 103–110, doi:10.1006/EESA.1999.1777.
25. Xiao, Y.; Vijver, M.G.; Chen, G.; Peijnenburg, W.J.G.M. Toxicity and accumulation of Cu and ZnO nanoparticles in daphnia magna. *Environ. Sci. Technol.* **2015**, *49*, 4657–4664, doi:10.1021/acs.est.5b00538.
26. Jang, G.H.; Park, C.-B.; Kang, B.J.; Kim, Y.J.; Lee, K.H. Sequential assessment via daphnia and zebrafish for systematic toxicity screening of heterogeneous substances. *Environ. Pollut.* **2016**, *216*, 292–303, doi:10.1016/J.ENVPOL.2016.06.001.
27. Lin, S.; Lin, S.; Zhao, Y.; Nel, A.E. Zebrafish: An in vivo model for nano EHS studies. *Small* **2013**, *9*, 1608–1618, doi:10.1002/sml.201202115. Hua, J.; Vijver, M.G.; Richardson, M.K.; Ahmad, F.; Peijnenburg, W.J.G.M. Particle-specific toxic effects of differently shaped zinc oxide nanoparticles to zebrafish embryos (*Danio rerio*). *Environ. Toxicol. Chem.* **2014**, *33*, 2859–2868, doi:10.1002/etc.2758.
28. Berg, J.M.; Romoser, A.; Banerjee, N.; Zebda, R.; Sayes, C.M. The relationship between pH and zeta potential of ~ 30 nm metal oxide nanoparticle suspensions relevant to in vitro toxicological evaluations. *Nanotoxicology* **2009**, *3*, 276–283, doi:10.3109/17435390903276941.
29. Tiller, C.L.; O'Melia, C.R. Natural organic matter and colloidal stability: Models and measurements. *Colloids Surfaces A Physicochem. Eng. Asp.* **1993**, *73*, 89–102, doi:10.1016/0927-7757(93)80009-4.
30. French, R.A.; Jacobson, A.R.; Kim, B.; Isley, S.L.; Penn, L.; Baveye, P.C. Influence of ionic strength, pH, and cation valence on aggregation kinetics of titanium dioxide nanoparticles. *Environ. Sci. Technol.* **2009**, *43*, 1354–1359, doi:10.1021/es802628n
31. User Guide Turbiscan Lab. Formulacion, Edition 4 Version 2.2.